Available online at www.sciencedirect.com
SCIENCE DIRECT
ELSEVIER
Coordination Chemistry Reviews 250 (2006) 710–727
COORDINATION CHEMISTRY REVIEWS
www.elsevier.com/locate/ccr

Review

Halogen acceptors in hydrogen bonding

Attila Kovács [a,*], Zoltán Varga [b]

[a] *Hungarian Academy of Sciences, Budapest University of Technology and Economics, Research Group of Technical Analytical Chemistry, H-1111 Budapest, Szt. Gellért tér 4, Hungary*
[b] *Institute of General and Analytical Chemistry, Budapest University of Technology and Economics, H-1111 Budapest, Szt. Gellért tér 4, Hungary*

Received 31 August 2004; accepted 4 April 2005
Available online 27 December 2005

Contents

Abstract

This review provides a comparative assessment of hydrogen bonding (HB) interactions with halogen (X) acceptors. Based on the data available in the literature we selected various inter- and intramolecular systems, for which (possibly) all the four halogen derivatives have been studied either by experimental or theoretical methods. Four main acceptor types have been considered in our assessment, viz., free X^- anions, halogens involved in M–X (M = transition metal), H–X and C–X bonds. The hydrogen donors in the HB systems (DH) included the simple H_2O, NH_3, HX, H_2 molecules, various alcohols, amines as well as aliphatic and aromatic CH groups. Among the molecular properties we focussed on the HB energy and structural characteristics (at the first place on the H···X distance), which are particularly informative on the HB propensities of the halogens. Where available, the shift of the DH stretching frequency (ν_{DH}) involved in the HB interaction is also discussed.

Keywords: Halogen acceptor; Hydrogen bonding; Hydrogen bonding energy; Geometry

1. Introduction

Although the primary attention within the huge area of hydrogen bonding (HB) is on the oxygen and nitrogen acceptors functioning in essential systems like water and biological

* Corresponding author. Tel.: +36 1 4632278; fax: +36 1 4633408.
E-mail address: akovacs@mail.bme.hu (A. Kovács).

0010-8545/$ – see front matter © 2005 Elsevier B.V. All rights reserved.
doi:10.1016/j.ccr.2005.04.031

molecules, interactions involving halogen acceptors have been reported from the early years of HB research [1]. In fact, the (probable) first use of the term "hydrogen bond" is connected with a halogen acceptor [2] in the discussion of bonding in the $[F–H–F]^-$ anion by Pauling [3]. Halogen acceptors in strong HB interactions often appear as textbook examples (HF_2^-, KH_2F_3, etc.).

From the halogen group fluorine and chlorine are detected most frequently in HB due to the generally large partial negative charges in their compounds. The less electronegative heavier halogens bromine and iodine have weaker proton acceptor abilities. Therefore, except the anions and metal halides, their interactions have often been considered as van der Waals (vdW) interactions. This classification was based on the vdW cut-off criterion (1970s among crystallographers), requiring that the H···acceptor distance be substantially shorter than the sum of the vdW radii ($\sum$vdW) of H and the acceptor [2]. The criterion fails for many H···Br and H···I contacts being around $\sum$vdW of the interacting atoms [4]. Recently, the cut-off criterion was seriously criticised as being far too restrictive and misleading [2,4,5]. In fact, the forces establishing HB interactions do not terminate at any cut-off distance, hence an exact border cannot be drawn between HB and vdW interactions. Rather, H···acceptor distances near $\sum$vdW should be considered as HB if the directions are also appropriate [2] distinguishing from vdW contacts, where no directionality is required.

The directionality of HB is governed by the electron density distribution around H and the acceptor. The depletion of the electron density on the opposite side of the D–H bond would favour a linear D–H···A (D–H = hydrogen donor; A = hydrogen acceptor) HB arrangement. On the other hand, the rich electron density around A in the direction of the lone pairs would prefer a H···A–Z (Z = any atom) angle of around 110°. Such angular preferences have been revealed in HB systems both in the gas and solid phases [2,4–7]. Even in crystals, where the angles can be distorted by weak forces, the linear D–H···A angles are statistically favoured over bent ones and the angular cut-off is usually set at >90° [8].

Reports on HB to halogen acceptors are less frequent than those to oxygen and nitrogen and describe mostly strong interactions to halide ions and metal halides [2]. The goal of our review is an assessment of HB interactions with halogen acceptors. We selected inter- and intramolecular systems, for which data are available for (possibly) all the four halogens. The molecular properties in our focus are the HB energy and structural characteristics (such as the H···A distance) being particularly informative on the HB propensities of the halogens. Where data are available, the discussion is extended to the shift of the DH stretching frequency (ν_{DH}) upon the interaction. Our assessment is primarily based on the most recent literature data from thermodynamic, crystallographic (neutron and X-ray diffraction), quantum chemical and vibrational spectroscopic studies. Note that several simple HB systems have been repeatedly investigated during the past decades taking advantage of improvements in the experimental and theoretical methods. In such cases, we do not intend to list the complete literature of the topic, instead, we focus on the most reliable recent data.

In order to retrieve lacking data in some important series of hydrogen-bonded compounds we performed quantum chemical calculations with the Gaussian '98 program [9]. These computations were carried out at the MP2/6-311++G(d,p) level using quasi-relativistic effective core potentials (ECP) for Br and I [10]. The valence basis set of the ECPs was extended by a single set of d-polarisation functions [11]. Our computed energies listed in the paper are corrected for zero-point vibrational energies (ZPE) obtained at the same level and – except for the intramolecular interactions – for basis set superposition error (BSSE).

Note that several books and comprehensive review papers on HB are available including also (mostly structural) data on halogen acceptors. A general overview of hydrogen bonding is given by Jeffrey in his book "An Introduction to Hydrogen Bonding" [2]. Theoretical data on HB of smaller systems prior to 1996 are collected in the book of Scheiner [7]. General characteristics of HB in the solid state are summarised by Steiner [12], whereas weak hydrogen bonds in the solid state are assessed in the book of Desiraju and Steiner [4]. Binding enthalpies and entropies of several hydrogen-bonded complexes and clusters are available in the NIST WebBook database [13].

The most comprehensive source of information on hydrogen-bonded structures in the solid phase is the Cambridge Structural Database (CSD, Ref. [14]). Several statistical analyses based on CSD appeared for the HB interactions of fluorine [15–20] and chlorine [19,21–24]. The rare data on Br and I acceptors did not permit an analysis of these interactions until recently. The first CSD searches on the latter two acceptors were reported in 1999 by Desiraju and Steiner [4] and by Brammer et al. [25]. In recent years, two additional studies based on CSD have been published: Neve and Crispini studied specifically C–H···Br–M interactions (M = metal) [26] while the analysis of van der Berg and Seddon included C–H···X interactions of all the four halogens [19].

2. Methods important in hydrogen bonding research

In this section, we briefly introduce the methods frequently applied in HB research. Note that a complete description of the methods is beyond the scope of this review. Instead, we focus here on their characteristics, advantages and disadvantages from the point of view of HB interactions.

2.1. Experimental methods for gas-phase studies

Isolated hydrogen-bonded complexes can be investigated by various gas-phase methods. Quantitative information on the structure is provided by electron diffraction and microwave spectroscopy. However, these methods (particularly microwave spectroscopy) are limited to small molecules only. Infrared (IR) spectroscopy is a simple but effective tool for identifying and characterising HB interactions. In addition to the gas phase, this technique can be used for both liquid and solid samples. This is particularly advantageous for large molecules, which decompose upon vaporisation. Among liquids the solutions in apolar solvents are informative on the isolated hydrogen-bonded

system, as these solvents have only marginal influence on HB.

The most significant feature in the infrared spectrum is the shift of the ν_{DH} frequency, connected to the change of the D–H bond distance upon HB [27]. Particularly in the case of weak HB can we benefit from the accurate determination of the ν_{DH} frequency, representing an important advantage of vibrational spectroscopy.

On the basis of data on various organic and inorganic HB systems, the red-shift of the ν_{DH} frequency has been correlated with the H···A and D···A donor–acceptor distances [28]. In addition, a correlation of $\Delta\nu_{OH}$ with measured bond enthalpies has been reported for O–H···O bonds [29]. However, more accurate crystal structure and computed data recently showed deviations (exceeding the uncertainties of the data) from a smooth relationship [2]. Moreover, the correlation was poor for weak HB interactions, particularly for those with C–H donors. Note that in some weak HB systems, an anomalous shift of the ν_{DH} frequency to higher wavenumbers (blue shift) was observed parallel with a marginal shortening of the D–H bond [30].

As the bands of the hydrogen-bonded and non-hydrogen-bonded systems appear at different wavenumbers in the IR spectrum, IR spectroscopy is well suited to study their equilibrium in the gas phase. The free energy and bonding enthalpy of the hydrogen bond can be determined from the van't Hoff plots of equilibrium constants obtained from temperature variable measurements. Limitations of the method appear in the case of overlapping bands and in the assumed identical absorption coefficient of the hydrogen-bonded and non-hydrogen-bonded species.

Additional, although less distributed, experimental methods for gas-phase equilibrium studies are high-pressure mass spectrometry [31,32] and ion cyclotron resonance mass spectrometry [33]. Vibrational predissociation spectroscopy connected to a mass spectrometer can be used to identify the mass-selected hydrogen-bonded species and to gain useful information on their vibrational properties [34,35].

2.2. X-ray and neutron diffraction

In the solid phase, neutron diffraction and X-ray diffraction are the primary tools in HB research. Locating the position of the hydrogen atom in the hydrogen bond, they give unambiguous information on the existence and strength of the interaction. Modern diffractometers with their associated commercial software packages have made X-ray and neutron crystal structure analysis an almost foolproof analytical procedure, providing not only the atomic coordinates, but also the equally important thermal motion parameters. From the two methods, X-ray diffraction is feasible and X-ray diffractometers belong to the basic instruments in molecular structure research. In contrary, neutron diffractometers require a neutron source, only available from national or international centers. Another advantage of X-ray diffraction is the shorter data collection time, while the neutron diffraction technique provides a more accurate determination of the positional parameters of hydrogen. A detailed discussion of the advantages and disadvantages of the two diffraction methods is given by Finney [36]. The crystal structure data of inorganic and organic compounds are collected in the Cambridge Structural Database [14].

The primary information on HB from diffraction studies are the distances and bond angles of the D–H···A–Z moiety. Most informative on the strength of HB is the H···A distance and the elongation of the D–H interaction. The latter parameter is less straightforward in the case of weak interactions, where the change of the D–H bond falls in the magnitude of experimental errors. In the case of moderate and weak hydrogen bonds the normalisation of the angular distribution effects is important as the D–H···A bond angle is easily bent from linearity, the bent bonds being entropy favoured. After application of the cone correction method [37] the distribution of the hydrogen bond angles cluster around the theoretically optimum value of 180°.

2.3. Quantum chemical computations

Quantum chemical computations gain increasing importance in HB research, particularly in the study of weak interactions. The main advantage of the computations is that, in principle, they model the isolated hydrogen-bonded system. This is particularly important for weak HB, where the characteristics of the weak H···X interaction are difficult to separate from other effects in condensed phases. In addition, simple approaches can be applied in the computations to assess the effect of solvent and that of neighbours in the crystal [38,39].

Several properties of HB can be obtained from quantum chemical computations, viz., full geometry, energy, molecular vibrations, detailed bonding interactions (electrostatics, polarisation, exchange repulsion, charge transfer and dispersion [40]). From the above properties, the bonding interactions can be investigated only by theoretical methods. Similarly, computations are the only tools to determine the HB energy of systems not suited for gas-phase experimental studies.

Ab initio calculations have been applied to hydrogen-bonded systems since the late 1960s [41]. While the early low-level works gave only qualitative information on some characteristic HB features, today the accuracy of the computational methods can approach that of the experiments [7]. It was made possible by the dramatic progress in computational chemistry including the development of new theoretical models, improvements in algorithms, and the advent of larger and faster computing machines. Despite of these developments, truly sophisticated theoretical levels can still only be applied for small molecules.

Selection of the theoretical level is very important in the computation of weak interactions like HB. Correlated wavefunctions and basis sets of at least double-zeta quality with polarisation functions on all atoms and diffuse functions on non-hydrogen atoms were found to be necessary to produce reasonable binding energies and reduce the basis set superposition error. As a minimum theoretical level for HB studies, the second-order Moller–Plesset theory (MP2 [42]) in conjunction with a 6-31+G(d,p) basis set has been recommended [43,44]. From density functional theory (DFT) methods, those

incorporating the hybrid exchange functional of Becke [45] were found to be adequate, but the use of large basis sets was suggested [46]. The most popular density functional in HB research is presently the Becke3–Lee–Yang–Parr exchange-correlation functional (B3LYP [45,47]). The requirements are more rigorous for weak HB interactions, where the dispersion term becomes important beside the small electrostatic one [4]. In such cases DFT is principally deficient due to the inability to account for dispersion forces [48].

Computation of the heavier halogens Br and I deserves special attention because of their large number of electrons and the relativistic effects. Both difficulties can be solved by using relativistic effective core potentials (ECP), the two most popular ones being those of Wadt and Hay [49] and Bergner et al. [10]. Polarisation functions for these ECPs are also available in the literature [11,50,51].

Comparison of experimental and computed data, however, should be done with caution. Experimental and computed results have generally different physical meanings [52]. The thermal motions are generally not included in the computed data whereas they appear in both the experimental geometrical parameters and binding enthalpy. The computed vibrational frequencies are usually obtained using the harmonic approximation, while the experimental values include the anharmonic effects. Therefore, a very good agreement occasionally found between experiment and theory can be illusory and is likely a result of fortunate cancellation of errors. Data from different computations can suffer from the different approximations involved in the various theoretical levels. All these influence the absolute values of the determined molecular parameters. More reliable are differences between the energies, geometrical parameters or vibrational frequencies of related compounds, e.g., between the hydrogen-bonded and non-hydrogen-bonded isomers or between similar hydrogen-bonded derivatives.

3. Intermolecular hydrogen bonding interactions

3.1. Anionic (X^-) acceptors

Halide anions form very strong HB interactions, as the negatively charged X^- is a very good proton acceptor. There are many data available on the small hydrogen-bonded complexes that are stable enough for gas-phase experimental investigations.

3.1.1. Hydrogen bihalides [X–H–X]$^-$

The hydrogen bihalide anions have a linear structure with $D_{\infty h}$ symmetry. The potential energy curve of the asymmetric stretching is rather flat in the proximity of the minimum in the case of heavier halogens (Cl, Br, I) leading erroneously to $C_{\infty v}$ double-well potential at less sophisticated quantum chemical levels [7]. The binding enthalpies and X–H distances of the [X–H–X]$^-$ bihalides are given in Table 1.

Comparison of the dissociation enthalpies and X–H distances in the [X–H–X]$^-$ anions to those of the XH molecules shows that the H···X interaction is considerably weaker in [X–H–X]$^-$. The dissociation enthalpies of an X–H bond in [X–H–X]$^-$ are ca. 25% of those of HX, whereas the X–H distances are longer by 20–25% in the bihalide anions. The bonds in [X–H–X]$^-$ are far below the sum of the van der Waals radii ($\sum$vdW) of X and H, indicating the very strong character of HB.

Table 1
Binding enthalpies (kJ/mol) and X–H bond distances (Å) of [X–H–X]$^-$ and XH species

	F^-	Cl^-	Br^-	I^-
[X–H–X]$^-$				
ΔH°	191.4 ± 6.7[a], 187.5[b]	96.7 ± 4.2[c], 100.9[b]	87.5 ± 4.2[d], 90.4[b]	71.1 ± 4.2[d], 54.9[e]
X–H	1.13886[f], 1.141[b]	1.57332[f], 1.556[b]	1.703[b]	1.910[e]
XH[g]				
ΔH°	569.87	431.62	366.35	298.407
X–H	0.91681	1.27455	1.41444	1.60916
$\sum$vdW[h]	2.67	2.95	3.05	3.16

[a] From energy-resolved collision-induced dissociation measurements in a flowing afterglow-triple quadrupole instrument [56].
[b] From equilibrium measurements by ion cyclotron resonance mass spectrometry for X = F and Cl [33].
[c] From equilibrium measurements by high-pressure mass spectrometry [57].
[d] Computed at the CCSD(T)/aug′-cc-pVTZ level. The computed energy was not corrected for BSSE [58].
[e] Computed in the present study at the MP2/6-311++G(d,p) level using quasi-relativistic ECP for Br and I [10,11]. The given energy is corrected for ZPE and BSSE.
[f] From rotational constants obtained by infrared diode laser spectroscopy: X = F (experimental error: ±0.00007 Å) [59], X = Cl (experimental error: ±0.00006 Å) [60].
[g] Bond dissociation energies and bond distances of the XH compounds [61].
[h] Sum of the van der Waals radii of H and X [62].

The bonding in the [X–H–X]$^-$ (X = F, Cl, Br) anions has recently been analysed by Berski and Latajka by means of a topological analysis of the electron localisation function [53]. In agreement with previous suggestions [54,55], their study revealed the considerable covalent character of the F–H bond in [F–H–F]$^-$. In accordance with the lower electronegativity of the heavier halides, the properties of the electron localisation function referred to a covalent nature of the X–H bond in [X–H–X]$^-$ increasing from X = F to Br [53].

3.1.2. Small halide complexes

Hydrogen-bonded complexes of halide ions with several small hydrogen donor molecules (DH = H_2O, alcohols, NH_3, C_2H_2, CH_4, H_2, etc.) have been observed and characterised by gas-phase experimental and quantum chemical methods. Due to the small size of the donors and the free space around the X^- anion, larger clusters can also be formed with coordination of additional donor molecules to X^- in the DH···X^- complex. These clusters are well suited to model ion–solvent interactions governing the structural and energetic properties of electrolyte solutions, hence the large interest in these systems. Especially the water···X^- interaction is important due to the ubiquitous presence of halide ions in aqueous chemistry.

The bonding enthalpies and H···X^- distances of the DH···X^- complexes are compiled in Table 2. Important features of the larger clusters formed by additional DH-coordination will be included in the discussion below.

Table 2
Bonding enthalpies (kJ/mol) and hydrogen bond lengths (Å) of selected D—H···X⁻ hydrogen-bonded complexes

DH	F^-	Cl^-	Br^-	I^-
H_2O				
ΔH°	97.51 ± 8.37[a]	61.52 ± 2.51[b]	48.96 ± 1.67[b]	43.11 ± 1.26[b]
H···X⁻	1.365[c]	2.151[d]	2.378[e]	2.805[f]
CH_3OH				
ΔH°	123.88 ± 4.18[g]	73.24 ± 1.26[h]	60.68 ± 0.42[h]	49.80 ± 0.84[h]
H···X⁻	1.339[i]	2.079[i]	2.42[j]	2.588[k]
EtOH				
ΔH°	135.59 ± 2.93[h]	74.91 ± 1.67[h]	59.00 ± 0.84[h]	54.41 ± 0.84[h]
i-PrOH				
ΔH°	140.20 ± 2.93[h]	81.19 ± 0.84[h]	60.26 ± 0.84[h]	54.82 ± 0.82[h]
H···X⁻	1.374[i]	2.190[i]	2.346[k]	2.677[k]
t-BuOH				
ΔH°	139.78 ± 2.93[h]	84.54 ± 1.67[h]	66.12 ± 0.84[h]	54.82 ± 1.26[h]
NH_3				
ΔH°	46.0 ± 4.2[l]	34.32 ± 0.42[m]	32.22 ± 0.42[m]	30.97 ± 1.26[m]
H···X⁻	1.617[k]	2.290[n]	2.572[k]	2.875[k]
C_2H_2				
ΔH°	100.9[o]	43.9[o]	36.12 ± 0.04[p]	29.31 ± 0.88[q]
H···X⁻	1.054[o]	2.253[o]	2.4800[q]	2.7626[q]
CH_4				
ΔH°	28.04 ± 0.84[r]	15.90 ± 0.84[r]	12.97 ± 0.84[r]	10.88 ± 0.84[r]
H···X⁻	1.88[r]	2.66[r]	2.887[k]	3.185[k]
H_2				
ΔH°	18.8[s]	5.84[t]	4.37[t]	3.03[t]
H···X⁻	1.678[u]	2.841[k]	2.983[k]	3.297[k]
$\sum$vdW[v]	2.67	2.95	3.05	3.16

[a] From gas-phase equilibrium measurements by high-pressure mass spectrometry [63].
[b] From gas-phase equilibrium measurements by pulsed electron beam high-pressure mass spectrometry [32].
[c] From MP2/aug-cc-pVTZ calculations [64].
[d] From MP2/6-311++G(d,p) calculations [65].
[e] From MP2/6-31++G(d,p) calculations [66].
[f] From MP2/6-311++G(d,p) calculations using relativistic ECP [67] for I [34].
[g] From gas-phase equilibrium measurements by high-pressure mass spectrometry [31].
[h] From gas-phase equilibrium measurements by high-pressure mass spectrometry [68].
[i] From MP2/6-311+G** calculations on the CH_3OH complexes and from B3LYP/6-311++G** calculations on the *i*-PrOH complexes [69].
[j] From MP2/D95 calculations [70].
[k] Computed in the present study at the MP2/6-311++G(d,p) level using quasi-relativistic ECP for Br and I [10,11].
[l] Estimated on the basis of the observed trend in the X = F—I series and simple electrostatic model calculations [71].
[m] From gas-phase equilibrium measurements by high-pressure mass spectrometry [71].
[n] From MP2/aug-cc-pVTZ calculations [72].
[o] From CCSD(T)/aug-cc-pVQZ calculations [73]. The entry under ΔH° for X = F^- is the equilibrium bond dissociation energy (without ZPE correction) with respect to the educts F^- and HCCH.
[p] From vibrational predissociation spectroscopy [74].
[q] From CCSD(T)/aug-cc-pVQZ calculations using ECP with valence basis of similar quality for I [75]. The ΔH° value of $C_2H_2\cdots I^-$ is based on the computed dissociation energy, corrected empirically by the observed difference between the experimental and computed data for $C_2H_2\cdots Br^-$ [75].
[r] ΔH° from gas-phase equilibrium measurements by high-pressure mass spectrometry, H···X⁻ from B3LYP/6-31+G* calculations [76].
[s] From CCSD(T)/VQZP calculations [77].
[t] From vibrational predissociation spectroscopy [35].
[u] From QCISD(T)/6-311++G(2df,2pd) calculations [78].
[v] Sum of the van der Waals radii of H and X [62].

The data in Table 2 reflect quantitatively the HB propensities of the different DH donors with halide ions. The strength of the hydrogen bond varies parallel with the acidity of the DH hydrogen. The strongest interactions appear with DH = *i*-PrOH and *i*-BuOH, although being weaker by 15–25% than in the respective $[X–H–X]^-$ bihalides (cf. Table 1). Among the DH donors listed in Table 2, the interaction is the weakest (by one order of magnitude) with the least acidic H_2. The H···X⁻ distances are generally in good agreement with the bonding enthalpies. Except for the $CH_4\cdots I^-$ and $H_2\cdots I^-$ complexes, they are below the $\sum$vdW value. We note the larger computed H···X⁻ distances in the *i*-PrOH complexes with respect to CH_3OH in contrast

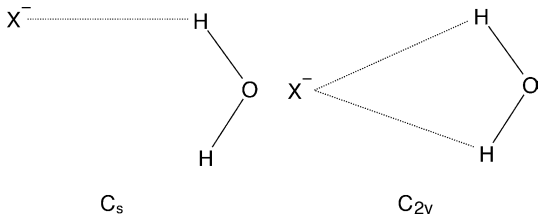

Fig. 1. Characteristic structures of water···X^- complexes.

to the stronger HB in the former complexes. In the cases of X = Cl^-, Br^- and I^-, the difference is around 0.1 Å, well over the expected deviation due to the different computational level for the *i*-PrOH and CH_3OH complexes of Cl^- and Br^-, while the two I^--complexes were calculated at the same level. The longer *i*-PrOH···X^- distance may likely be attributed to the larger steric effects of *i*-PrOH.

Quantum chemical calculations on the 1:1 complexes of water and X^- indicated the single-coordinated C_s isomer (Fig. 1) being the global minimum on the potential energy surface, whereas the C_{2v} isomer proved to be a somewhat higher lying saddle-point [34,64–66,79,80]. These computed results were supported by the IR spectra of HOH···Cl^- [65] and HOH···I^- [34] showing free and bound OH stretching vibrations in agreement with only one hydrogen of the water molecule involved in HB.

When increasing the number of solvent molecules around X^-, a competition occurs between the solute–solvent and solvent–solvent HB interactions. F^- prefers to be surrounded by water molecules because the HOH···F^- interaction is somewhat stronger than the H_2O···H_2O interaction. Further addition of H_2O ligands to the HOH···F^- complex is accompanied by smaller enthalpies of hydration than that of the first step. The ΔH° values of the additional hydration steps are smaller by 17% ($n = 2$) to 53% ($n = 6$) [32].

Compared to F^-, the importance of the H_2O···H_2O interaction is increased in the clusters of the heavier halide ions (Cl^-, Br^-, I^-) with H_2O. In these systems X^- favours a connection to the surface of the hydrogen-bonded $(H_2O)_n$ cluster and, if n is small enough, the other side of X^- can be unoccupied [66]. This surface-bound structure was supported by spectroscopic studies [34,65]. On the other hand, computations at the MP2/6-311++G(d,p) level indicated small energy differences between the various cluster structures [81–84]. This points to a possible interchange of the stability order at higher temperatures upon to the entropy effect.

The complex formation of halide anions with small alcohols (CH_3OH, EtOH, *i*-PrOH, *t*-BuOH) has been investigated recently by McMahon et al. [68] using pulsed-ionisation high-pressure mass spectrometry. They determined the enthalpies of formation of several smaller clusters $X^-(HOR)_n$ ($n = 1$–3) and reviewed the previous literature on the subject. The consistent results of McMahon et al. compiled in Table 2 (for earlier data see Ref. [68]) reflect well the trends within both the halide and alcohol groups. The bonding enthalpies increase from DH = CH_3OH to *i*-BuOH parallel with the deprotonation enthalpies of the alcohols. The stronger HB in CH_3OH···X^- with respect to HOH···X^- is also supported by the measured red-shifts of the OH stretching frequencies (e.g., 386 cm^{-1} in CH_3OH···I^- versus 300 cm^{-1} in HOH···I^- [85]).

The two-dimensional (H···X^- distance versus O–H···X^- angle) potential energy surfaces of the CH_3OH···X^- complexes indicated a nearly symmetric, hydrogen-bonded surface for X = F. The surface of complexes with X = Cl, Br and I becomes more asymmetric due to the increased importance of other (ion–dipole, ion–induced dipole) interactions [69]. The computed flat potential energy surfaces also confirmed the "floppy" nature of the motion of the halide ion around the alcohol molecule.

McMahon et al. assessed the performance of three popular quantum chemical levels (G2, MP2/6-311+G(d,p), and B3LYP/6-311+G(d,p)) to estimate the enthalpies of formation of $(ROH)_n$···X^- [68,69]. The G2 values differed by 7.5 kJ/mol from experiment, which is within the generally found accuracy of the G2 method (8–12 kJ/mol). The B3LYP/6-311+G(d,p) level performed somewhat worse, these data deviated up to 12 kJ/mol from experiment.

The ΔH° values of the second and third DH ligands in the $X^-(HOR)_n$ clusters ($n = 2, 3$) are considerably smaller than ΔH° of the first DH [68]. The decrease is most pronounced in the fluorides (ca. 40% for the second and ca. 50% for the third ligand) in agreement with the large steric interactions around the small F^- ion. Down the halogen group the weaker steric effects result in less drastic decrease, e.g., in the iodide clusters ca. 15% and 30% for bonding of the second and third DH, respectively.

Fewer examples of NH_3···X^- systems are known than for complexes of H_2O and alcohol ligands. The most extensive studies have been performed for the NH_3···Cl^- complex using photoelectron spectroscopy [86], high-pressure mass spectrometry [71], infrared spectroscopy [72] and quantum chemical calculations [72,86]. For the bromide and iodide complexes the association enthalpies have only been determined by high-pressure mass spectrometry [71]. The bonding enthalpy of NH_3···F^- has been estimated on the basis of the trend in the halide group and simple electrostatic model calculations [71]. The bonding enthalpies compiled in Table 2 reveal by ca. 50% weaker interaction in NH_3···F^- with respect to HOH···F^-. The relative strength of the NH_3···X^- complexes with respect to the HOH···X^- ones is somewhat larger in the heavier halides (up to ca. 75% in the case of X = I).

Quantum chemical calculations on NH_3···Cl^- at the MP4SDTQ/aug-cc-pVTZ//MP2/aug-cc-pVTZ level (using ZPE and BSSE corrections) revealed the preference of the monodentate C_s structure presented in Fig. 2 over the tridentate C_{3v} structure by 8.9 kJ/mol [72]. The bidentate C_s structure proved to be a transition state on the potential energy surface. Analysis of the NH stretching vibrations in the IR spectrum of NH_3···Cl^- supported the preference of the monodentate structure [72].

Among the C_2H_2···X^- complexes experimental bond energetic data are only available for C_2H_2···Br^- [74]. In addition, sophisticated quantum chemical calculations using the CCSD(T) method have been performed for all the four halide complexes [73,75]. Both the spectroscopic and computational

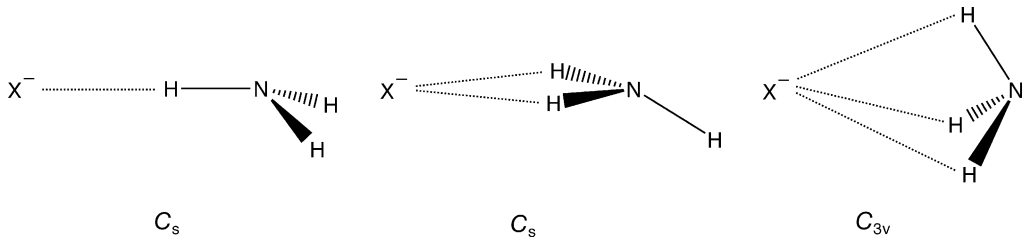

Fig. 2. Characteristic structures of the $NH_3\cdots X^-$ complexes.

studies supported a linear structure of the complexes with only one acetylene hydrogen attached to X^-.

The equilibrium structure of the three heavier halides (X = Cl, Br, I) corresponds to $C_2H_2\cdots X^-$ [73,75]. There is, however, contradicting information on the equilibrium structure of the $C_2H_2\cdots F^-$ complex in the literature. Its formation among the elimination products of vinyl fluoride was proposed by Roy and McMahon [87] and supported later by Rabasco and Kass on the basis of reactivity studies (hence not observed directly) and ab initio computations [88]. HF/6-31+G(d) and MP2/6-31+G(d) computations resulted in reasonable bond dissociation energy of ca. 80 kJ/mol and $H\cdots F^-$ distance around 1.5 Å [88]. The $C_2H_2\cdots F^-$ structure of as the reaction product of C_2H_2 + CsF deposited in Ar-matrix was verified on the basis of the modest red-shift of the CH stretching vibration [89]. However, high-level CCSD(T)/aug-cc-pVQZ [73] and DFT computations [90] did not find any $C_2H_2\cdots F^-$ minimum on the potential energy surface, instead, the geometry optimisations converged to a linear $HC_2^-\cdots HF$ structure. The latter computed results are particularly surprising, because the equilibrium proton affinity of the acetylide anion is larger by 30.9 kJ/mol than that of F^- [73]. The proton affinity, however, refers to the isolated HC_2^- and F^- anions, whereas in the $[HC_2\cdots H\cdots F]^-$ complex the composite bonding interactions determine the energy profile. The different results from the low- and high-level computations imply a flat potential energy curve of the proton transfer between HC_2^- and F^-. The discrepancy between the high-level computations and the matrix-IR study of Simmonett et al. [90] can additionally be explained by the different conditions in the two studies. The computations model the isolated $[HC_2\cdots H\cdots F]^-$ anion, whereas in the Ar-matrix the Cs^+ ions were also around and could stabilise the $C_2H_2\cdots F^-$ structure.

The considerable energy gain can facilitate the formation of $(C_2H_2)_n\cdots X^-$ clusters with spherical arrangement of the acetylene ligands around X^-. The IR spectra of the clusters of X = Cl, Br and I showed that the first solvation shell of Cl^- includes six to eight acetylene [91], that of Br^- six to seven acetylene [35]. For the $(C_2H_2)_n\cdots I^-$ clusters (n_{max} = 4) only the first solvation shell could be observed [92].

Methane is a very weak C–H donor, yet it can form hydrogen-bonded complexes up to small clusters with the strong X^- acceptors. The bonding enthalpies have been determined by gas-phase equilibrium measurements using pulsed electron-beam high-pressure mass spectrometry [76]. Quantum chemical computations at the MP2 level gave somewhat lower binding energies [93,94].

The computations indicated that from the three possible geometries (monodentate, bidentate, tridentate, cf. Fig. 3) only the linear monodentate structure is a true minimum on the potential energy surface. This C_{3v} structure of $CH_4\cdots F^-$, $CH_4\cdots Cl^-$ and $CH_4\cdots Br^-$ complexes was supported by vibrational predissociation spectroscopy in a low-energy tandem mass spectrometer [94,95]. The relatively low binding energies of the $CH_4\cdots X^-$ complexes are also reflected in the small red-shifts of the C–H stretching frequencies (380, 40 and 30 cm^{-1} for X = F, Cl and Br, respectively [95]). They are smaller by one order of magnitude than the corresponding ν_{OH} shifts observed for the $HOH\cdots X^-$ complexes (2000, 570 and 430 cm^{-1} for X = F, Cl and Br, respectively) [96,97].

Among the $(CH_4)_n\cdots X^-$ systems the fluoride clusters (n = 1–4) have been observed and computed at the B3LYP/6-31+G* level [76]. The computations revealed symmetric structures: $D_{\infty h}$, D_{3h} and T_d for n = 2, 3 and 4, respectively. The experimental bonding enthalpies of the additional CH_4 ligands decrease by 13%, 19% and 26% for n = 2, 3 and 4, respectively, as compared to the bonding enthalpy of the $CH_4\cdots F^-$ complex. Parallel, the computations indicated $H\cdots F^-$ distances increasing from n = 1 to 4 [76].

$H_2\cdots X^-$ dimers of all the four halogens have been observed by vibrational predissociation spectroscopy [98–100]. The spectra are indicative of a linear structure with X^- connected to one of the hydrogens only. On the other hand, quantum chemical calculations revealed a flat potential energy surface for the rotation of H_2. Hence, the system is rather floppy

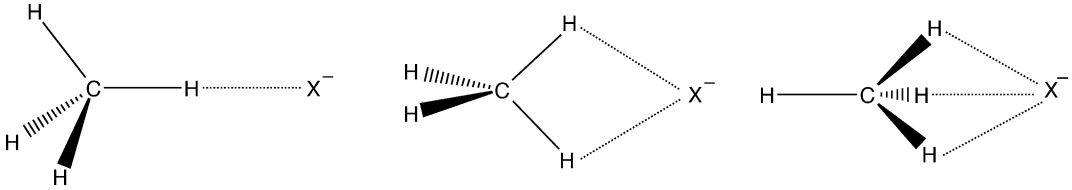

Fig. 3. Possible structures of $CH_4\cdots X^-$ complexes.

facilitating an interchange of the bonding and terminal H atoms [35,78].

The hydrogen bond in $H_2\cdots F^-$ is quite strong as evidenced also by the 940 cm^{-1} red-shift in the H–H stretching vibration [100]. The HB interaction is much weaker in the $H_2\cdots Cl^-$, $H_2\cdots Br^-$ and $H_2\cdots I^-$ complexes showing $\Delta\nu_{HH} = 150$, 111 and 54 cm^{-1}, respectively [98,99].

Larger clusters of such systems have been reported only for $(D_2)_n\cdots F^-$ ($n = 1$–6) and $(D_2)_n\cdots Cl^-$ ($n = 1$–3) on the basis of vibrational predissociation spectroscopic studies [101]. The spectra were compatible with roughly equivalent D_2 ligands attached end-on to the central anion in the clusters. There were no signs of a second D_2 solvation shell up to $n = 6$ and 3 in the $(D_2)_n\cdots F^-$ and $(D_2)_n\cdots Cl^-$ clusters, respectively. The shift of the ν_{DD} frequency to the lower wavenumbers depends strongly on the size of the $(D_2)_n\cdots F^-$ cluster (e.g., 457 and 214 cm^{-1} for $n = 2$ and 6, respectively), whereas it changes within a few cm^{-1} only for the $(D_2)_n\cdots Cl^-$ clusters.

3.1.3. Halide complexes observed in the condensed phase

Structural data on HB complexes with larger DH donors are available from CSD. The most thorough analysis was performed by Steiner in 1998, who sorted the observed contacts by the character of the hydrogen donor [102]. Other (earlier and more recent) CSD studies [4,15–26] did not distinguish in such detail between various DH donors, therefore we discuss here selected results of Steiner (Table 3). They are the mean $H\cdots X^-$ distances for most of which a large number of contacts are available, justifying their reliability.

The most important conclusion from the data in Table 3 is, that the differences between the different halides agree well with the variation of the halide ionic radii from F^- to I^- (1.33, 1.81, 1.96 and 2.20 Å, respectively [61,103]). Note that the gas-phase and computed $H\cdots X^-$ distances for HB complexes with small DHs (Table 2) show deviations up to 0.35 Å from the solid-phase data. The difference may primarily be attributed to steric, crystal packing and additional intermolecular (e.g., HB) effects in the solid.

Regarding the proton donor groups, the data in Table 3 reveal the expected trend for the strength of the $H\cdots X^-$ interactions. It increases parallel with the acidity of DH pointing to the minor importance of solid-phase effects on the HB systems. The HB propensity of the various DH groups can be distinguished clearly: the $H\cdots X^-$ distances differ generally by 0.1–0.2 Å for a selected X^-. Among the listed DH groups the group of N–H donors shows smaller variations, indicating smaller differences in the acidic character within the group.

Table 3
Mean $H\cdots X^-$ distances (in Å, X = F, Cl, Br, I) with $D{-}H\cdots X^-$ angles >140° [102][a]

DH	F^-	Cl^-	Br^-	I^-
O–H donors				
H–O–H	1.71 (14)	2.237 (799)	2.400 (148)	2.66 (47)
$C(sp^3)$–O–H	1.58 (1)	2.150 (299)	2.310 (90)	2.55 (27)
O=C–O–H	1.50 (5)	2.044 (65)	2.20 (16)	2.42 (1)
N–H donors				
$-N(sp^2)H_2$	1.74 (2)	2.350 (314)	2.52 (77)	2.79 (30)
$-N^+H_3$	1.67 (3)	2.247 (467)	2.49 (88)	2.72 (29)
$>N(sp^2)H$	1.64 (5)	2.221 (256)	2.39 (40)	2.69 (20)
$>N^+H_2$	1.69 (1)	2.162 (312)	2.34 (63)	2.76 (1)
$(CC)N^+$–H	1.56 (2)	2.126 (174)	2.29 (39)	2.63 (3)
$(CCC)N^+$–H		2.079 (232)	2.29 (90)	2.54 (5)
C–H donors				
Cl_3C–H		2.39 (14)	2.62 (1)	2.84 (4)
C≡C–H		2.49 (8)	2.70 (5)	
$(NC)C(sp^2)$–H	2.18 (1)	2.64 (110)	2.74 (56)	2.99 (44)
$\sum$vdW[b]	2.67	2.95	3.05	3.16

[a] Distances are normalised, number of contacts are given in parentheses.
[b] Sum of the van der Waals radii of H and X [62].

As was shown above for the small halide complexes, the halide anion acceptors are favourable for HB interactions with more than one donor simultaneously. Multiple hydrogen bonds have been observed particularly at the heavier halogens with weak hydrogen donor C–H groups [102], where the large size of the halogen and the relatively long $H\cdots X^-$ distances are sterically favourable. The small and strong F^- acceptor is generally involved in a single hydrogen bond (especially if DH = OH or NH) being sterically less available for a second donor.

In competitive situations, where different types of donors coordinate to the acceptor, the stronger donor dominates. Representative examples are the propargyl ammonium halides (Fig. 4), in which the halide anions interact with three ammonium groups and with the acetylenic C–H of the propargyl residue [104]. In this structure the C≡C–$H\cdots X^-$ bonds (2.62, 2.75 and 2.96 Å for Cl^-, Br^- and I^-, respectively) are longer than the mean value given in Table 3, whereas the $N^+H_3\cdots X^-$ bonds are slightly shorter (2.19, 2.33 and 2.57 Å for Cl^-, Br^- and I^-, respectively) than observed generally (cf. Table 3). The structure reveals optimised $N^+H_3\cdots X^-$ interactions at the expense of the weaker C≡C–$H\cdots X^-$ ones.

We terminate this section with a characteristic host–guest interaction operating through HB to halide anions. Halide-receptor calix[4]pyrroles have the ability to capture a single

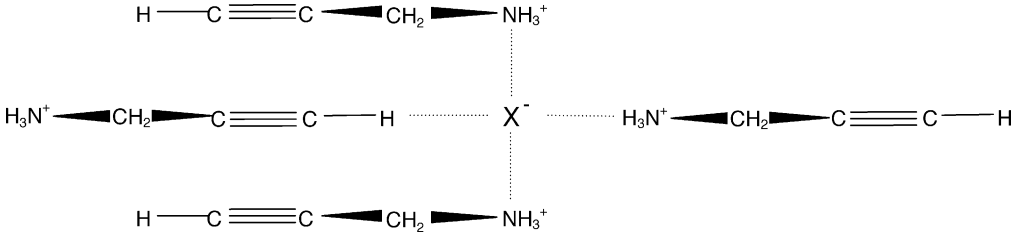

Fig. 4. HB interactions in crystalline propargyl ammonium halides [104].

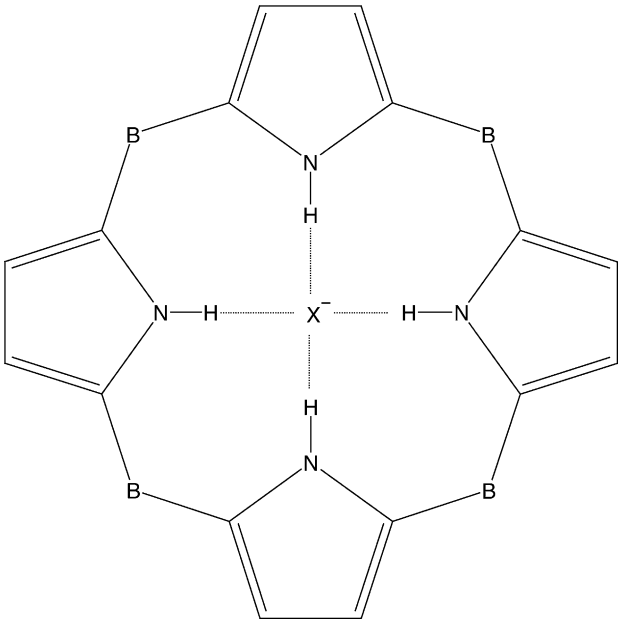

Fig. 5. Chemical structure of calix[4]pyrrole complexed with a halide anion. B = bridging moiety.

X^- by forming four equivalent N–H···X^- hydrogen bonds [105–110] (Fig. 5). Experimental binding constants of derivatives with $B = C(CH_3)_2$ indicate a substantially decreasing stability of the halide complex down the halide group [105]. In agreement with that, quantum chemical calculations at the B3LYP/LANL2DZ//HF/LANL2DZ level gave BSSE-corrected binding energies of 394.1, 259.0, 219.7 and 183.3 kJ/mol for the F^-, Cl^-, Br^- and I^- complex of calix[4]pyrrole ($B = CH_2$), respectively [111]. The flexibility of calixarenes facilitates the best arrangement for the capture of X^-, hence the strength of the interaction will be determined by the HB propensity of X^-.

3.2. M–X acceptors

Halogens bonded to transition metals (M) are good HB acceptors. This property is based on the strongly polarised character of the M–X bond resulting generally in an enhanced partial negative charge of the halogen. The phenomenon is known as metal-assisted HB [26]. Whereas a large number of structural data on H···X–M hydrogen bonds is available in the crystallographic literature, information on the HB energy of such systems is rare. Our literature search found only one example with consistent data on the whole halogen group: the bond strength of the intramolecular N–H···X–Ir interaction in mer-$[IrH_2X(pyNH_2)(PPh_3)_2]$ was found to be 21.8, 8.8, 7.5, <5.4 kJ/mol for X = F, Cl, Br and I, respectively, determined by NMR spectroscopy in solution [112].

A comprehensive search of CSD on H···X–M hydrogen bonds including the O–H, N–H and C–H donors has been performed by Brammer et al. [25]. The hydrogen-bond lengths were characterised by the mean normalised R_{HX} distances obtained from the formula $R_{HX} = d(H\cdots X)/(r_H + r_X)$, where $d(H\cdots X)$ is the measured H···X distance, r_H and r_X are the vdW radii of H and X, respectively. The advantage of the R_{HX} parameter is that, being the ratio of the H···X distance and ∑vdW, it provides a uniform clue for the strength of HB.

Table 4
Mean R_{HX}[a] normalised distances (Å) of H···X contacts

	F—M	Cl—M	Br—M	I—M
O—H[b]	0.703	0.799	0.820	0.868
N—H[b]	0.776	0.853	0.879	0.923
C—H[b]	0.943	0.975	0.982	0.997
C—H[c]	0.924	1.009	1.024	1.060

[a] $R_{HX} = d(H\cdots X)/(r_H + r_X)$, where $d(H\cdots X)$ is the measured H···X distance, r_H and r_X are the vdW radii of H and X, respectively.
[b] From Ref. [25]: $R_{HX} < 1.048$ Å and D—H···X > 110°.
[c] Evaluated in the present study from the data given in Ref. [19]: $d_{HX} < 7$ Å and D—H···X > 90°.

The results of Brammer et al. [25] given in Table 4 are in agreement with expected trends for the strength of HB based on the polarity of the D–H and X–M bonds with different D and X. Hydrogen bonds with metal fluorides are markedly shorter than those of their heavier halogen congeners. The preference for D–H···X linearity at short H···X separations was found to decrease in the order M–F > M–Cl > M–Br > M–I for the acceptors and in the order O–H > N–H > C–H for the donors [25]. In a recent CSD analysis of C–H···Br–M interactions Neve and Crispini found also a pronounced preference for linearity [26]. The directionality of the interactions supports that these C–H···X–M interactions (with X = Br and I), although the H···X distances are near the ∑vdW cut-off limit, can still be considered as weak hydrogen bonds instead of vdW interactions.

The analysis of Brammer et al. revealed H···X–M angles (X = Cl, Br, I) preferring values between 90° and 130° [25]. Regarding the N–H···X–M hydrogen bonds, for example, H···X–M angles within the range of 90–130° were found in 66.0%, 62.3% and 75.4% of all the observations with Cl, Br and I acceptors, respectively. On the other hand, the ratio found for X = F was 32.4% only. Rather, 64.1% of all the N–H···F–M contacts adopted H···X–M angles in the range of 130–160° [25]. The marked difference in the above angular preferences was attributed to the greater contribution of the axial p-orbital of the heavier halogens to the M–X bonding. Note that Neve and Crispini found a very weak anisotropy in the (C–)H···Br–M angle [26], much weaker than reported for interactions with the stronger donor OH and NH groups [25].

C–H···X–M interactions have been covered recently in the CSD search of van der Berg and Seddon [19]. Due to the different search criteria and data analysis process they reported somewhat different optimal lengths for the C–H···X hydrogen bonds than given by Brammer et al. [25]. The normalised R_{HX} values derived from the results of van der Berg and Seddon are included in the last line of Table 4. Nevertheless, the trend among the different M–X acceptors agrees with that reported by Brammer et al. [25].

3.3. H–X acceptors

The HX dimers and oligomers have been the subject of an extensive research. The lighter derivatives HF and HCl are

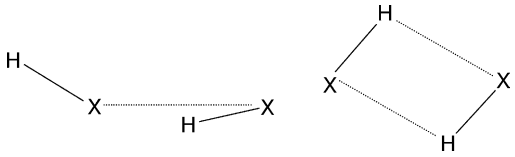

Fig. 6. The pseudolinear and cyclic structures of $(HX)_2$ dimers.

known to organise themselves as zig–zag chains in condensed phases [113]. A neutron diffraction study of the HI liquid at 253 K indicated no HB interaction, the average I···I distances being around 4.5 Å [114]. The dimers have been detected in the gas phase with various methods [113,115,116]. Molecular beam and microwave spectroscopic studies reported pseudolinear structures (cf. Fig. 6) for $(HF)_2$ [67] and $(HCl)_2$ [117], respectively. However, the large amplitude motions on the flat potential energy surface hampered the determination of the H···F and H···Cl distances. For detailed spectroscopic studies on the dynamical properties of the two dimers, see e.g., Refs. [118,119].

Due to their simplicity, the structure and potential energy surface of the homo- and heterodimers of HX have already been explored early by quantum chemical computations. Computations at both the Hartree–Fock [120,121] and MP2 [122] levels gave the pseudolinear structure preferred over the cyclic transition state (cf. Fig. 6), although the difference is very small (3.3 kJ/mol for $(HF)_2$ [120] and between 0.8 and 0.4 kJ/mol for $(HX)_2$ with X=Cl–I [122]).

The dissociation energies and H···X distances of the D–H···X–H homo- and heterodimers are given in Table 5. Because the H···X distances were not given in Refs. [122,124], we derived them from the geometrical data reported in the above studies. The dissociation energy and H···X distance of $(HF)_2$ indicate a considerable, whereas those of the other $(HX)_2$ compounds rather weak HB interactions. Note that the H···X distances with X = I acceptor are near the $\sum$vdW value, yet, these interactions show dissociation energies between 4.4 and 5.8 kJ/mol, ca. 25% of that of $(HF)_2$. The binding energies of the heavier $(HX)_2$ dimers, however, include a considerable contribution from dispersion forces beyond HB. The dipole–induced dipole and induced dipole–induced dipole interactions (based on the polarisability of the monomer) become particularly important in the dimers of HBr and HI, in which the polarised character of the H–X bond is decreased (cf. the dipole moment and polarisability data listed in Table 5). On the other hand, in the lighter $(HX)_2$ dimers the dipole–dipole interactions can make a substantial contribution to the binding energy. Altogether, the trend in the energy and geometrical data (HF > HCl > HBr > HI) seems to be determined primarily by the HB and dipole–dipole interactions.

The elongation of the X–H bonds and the red-shift of the ν_{XH} frequencies upon dimerisation are particularly interesting in the X = Cl, Br, I series. In agreement with the weak interaction, the X–H bonds are elongated by 0.002–0.004 Å with respect to the monomer values. In contrast to the expectations on the basis of the dissociation energies, however, the largest elongation (0.004 Å) was computed for $(HI)_2$, whereas the other two

Table 5
Dissociation energies (D_e, in kJ/mol) and H···X distances (Å) of D—H···X—H dimers (D, X = halogen) from quantum chemical calculations

Acceptor	DH			
	F	Cl	Br	I
F				
D_e[a]	19.1 ± 1.2 (12.4 ± 0.5)			
D_e[b]	20.9			
H···X[b]	1.873			
Cl				
D_e[a]		9.5 ± 1.0 (5.2 ± 0.3)		
D_e[c]		6.8	6.0	4.7
H···X[c]		2.562	2.606	2.797
Br				
D_e[c]		6.5	5.8	4.6
H···X[c]		2.722	2.749	2.944
I				
D_e[c]		5.8	5.4	4.4
H···X[c]		2.964	2.987	3.133
$\sum$vdW[d]	2.67	2.95	3.05	3.16
μ[e]	1.826178	1.1086	0.8272	0.448
α[e]	0.80	2.63	3.61	5.44

[a] Experimental dissociation energies (D_e) from absolute infrared intensities. ΔH° values are given in parentheses [123].
[b] From MP2/6-311++G(2d,2p) calculations including correction for BSSE [124].
[c] From MP2 calculations using an ECP with double-ζ valence basis sets augmented by diffuse sp and two sets of polarisation functions [122]. The D_e values lack ZPE, but include BSSE corrections.
[d] From Ref. [62].
[e] Dipole moments (μ, in Debye) and average electric dipole polarisabilities (α, in $\times 10^{-24}$ cm^3) [61].

dimers showed an effect of only 0.002 Å [122]. Similarly, the computed red-shifts of ν_{XH} are in disagreement with the trend in the dissociation energies. The largest effect was found in the $(HBr)_2$ dimer (88 cm^{-1}) whereas it was smaller in both $(HCl)_2$ (53 cm^{-1}) and $(HI)_2$ (36 cm^{-1}) [122]. The available experimental data are less suitable for comparison. For $(HCl)_2$ a red-shift of 29 cm^{-1} was measured in the gas phase [125], whereas for $(HBr)_2$ and $(HI)_2$ shifts of 60 cm^{-1} [126] and 54 cm^{-1} [116], respectively, in Ar-matrix. Beyond the obvious difference in the vapour and matrix-isolation conditions, the Ar-matrix may have slightly different effects on $(HBr)_2$ and $(HI)_2$, as they have different polarisabilities. Nevertheless, the computed and experimental trends agree for the latter two dimers.

Except for the microwave spectroscopic study of the HI···HF complex [127] suggesting a similar pseudolinear structure like found for the homodimers (cf. Fig. 6), only computational results have been reported for the D–H···X–H heterodimers. The computed dissociation energies and characteristic geometrical parameters of the heterodimers are intermediate of those of the homodimers [122]. On the basis of the data in Table 5 the nature of the proton-donor molecule seems to have a larger effect on the strength of interaction than that of the proton acceptor. Changing the donor results in a difference of up to 2.1 kJ/mol in the dissociation energy, whereas a change of the acceptor up to 1.0 kJ/mol only. In agreement with both the dipole moment

and polarisability data, the dissociation energies show a larger decrease between HBr and HI (both as donor and acceptor) than between HCl and HBr.

Elongation of the X–H bond upon dimerisation shows the same characteristics in the heterodimers like found in the homodimers: the elongation is 0.002 Å between HCl and HBr, 0.003 Å when HI is either donor or acceptor and 0.004 Å in $(HI)_2$ [122]. The observed geometrical and vibrational characteristics of the D–H···X–H homo- and heterodimers indicate, that in these compounds interactions different from the traditional HB may determine the lengthening of the donor X–H bonds and the red-shift of the ν_{XH} frequencies.

Except for $(HI)_4$, all the homotrimers and homotetramers of HX have been detected by matrix-isolation IR spectroscopy suggesting a cyclic structure for these species [128–134]. The exact geometries of the $(HX)_3$ and $(HX)_4$ species have been explored by computations [122,134–136]. Only one minimum was found on the potential energy surface corresponding to a C_{nh} ($n = 3, 4$) cyclic structure. The computed dissociation energies and geometrical characteristics revealed the importance of cooperative effects in strengthening the bonding interaction. In the X = Cl, Br, I series, the largest dissociation energies have been found for $(HCl)_n$ (22.2 kJ/mol in the trimer, 36.0 kJ/mol in the tetramer), somewhat weaker for $(HBr)_n$ (19.3 kJ/mol in the trimer, 30.6 kJ/mol in the tetramer) and much weaker for $(HI)_n$ (13.8 kJ/mol in the trimer, 20.5 kJ/mol in the tetramer) at the MP2 level [122]. The cooperativity results in a stabilisation of ca. 66% in $(HCl)_3$ and $(HBr)_3$, 76% in $(HCl)_4$ and $(HBr)_4$ whereas 55% in $(HI)_3$ and $(HI)_4$.

In addition to the above study, several computations have been performed on $(HF)_n$ oligomers at various levels of theory [134–137]. A meaningful comparison with the above discussed data of the heavier halides is hampered by the different level, therefore we note only some important characteristics from the extensive DFT study on $(HF)_{2–10}$ and $(HCl)_{2–6}$ by Guedes et al. [137]. The planar C_{nh} structure of the small oligomers is forced to break at $n \geq 7$ and ≥ 5 for $(HF)_n$ and $(HCl)_n$, respectively. Responsible for this are the dipolar and quadrupolar interactions competitive to HB. The cooperative effects increase till $n = 4$ in both $(HX)_n$, while after a short descending period they reach a limit in $(HF)_8$ and $(HCl)_6$.

3.4. C–X acceptors

Information on the bonding energies of C–X acceptors is rare. A few systems have been investigated by quantum chemical calculations and vibrational spectroscopy. On the other hand, numerous D–H···X–C contacts can be found in CSD. They have been the subject of several previous CSD analyses and reviews [4,15–24]. In the following, we discuss primarily systems for that energy data are available.

The CH_3X dimers represent weak complexes due to the very weak acidic nature of the C–H hydrogen. They can be produced by supersonic jet expansion and have been investigated by Nakata et al. by matrix isolation infrared spectroscopy [138–140]. The observed IR bands have been assigned on the basis of quantum chemical computations. The computations at the MP2/DZP and B3LYP/6-311++G(3pd,3df) levels found three characteristic structures on the potential energy surface (Fig. 7) [140,141]. The head-to-tail (C_{2h}) structure has H···X distances near $\sum$vdW of the interacting atoms. The head-to-head structure (C_s) was obtained only for $(CH_3Br)_2$ and $(CH_3I)_2$. The X···X distances are shorter by a few tenths of angstrom than $\sum$vdW, whereas the H···X distances are close to it. This implies that a marginal attractive interaction may appear between the halogens of the monomers facilitated by their large polarisability. In the linear (C_{3v}) structure (not found for CH_3I) the H···X distances are again near $\sum$vdW of the interacting atoms.

The C_{2h} structure was found to be the global minimum on the potential energy surface of all the CH_3X dimers with BSSE-corrected dimerisation energies of 6.5 (B3LYP/6-311++G(3pd,3df)), 12.5 (MP2/DZP) and 7.6 kJ/mol (MP2/DZP) for X = F, Br and I, respectively. (Note that the dimerisation energy of CH_3Cl was not given in Ref. [140].) The above results show the deficiency of DFT calculations for dispersion forces [48] important in interactions near the $\sum$vdW distance. This may be one of the main reasons that the B3LYP calculations did not find the less stable C_s structure of $(CH_3F)_2$

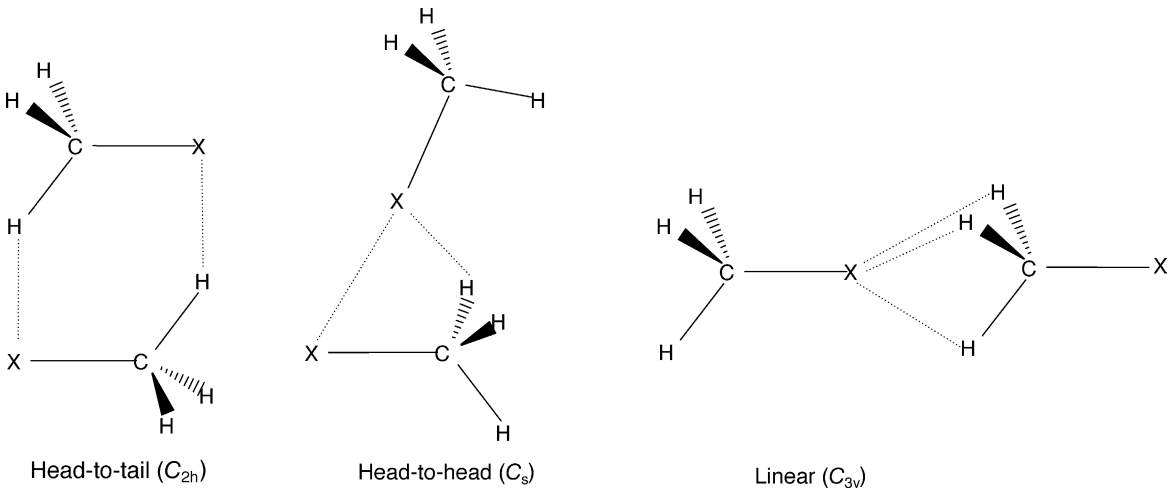

Fig. 7. Characteristic structures of $(CH_3X)_2$ dimers.

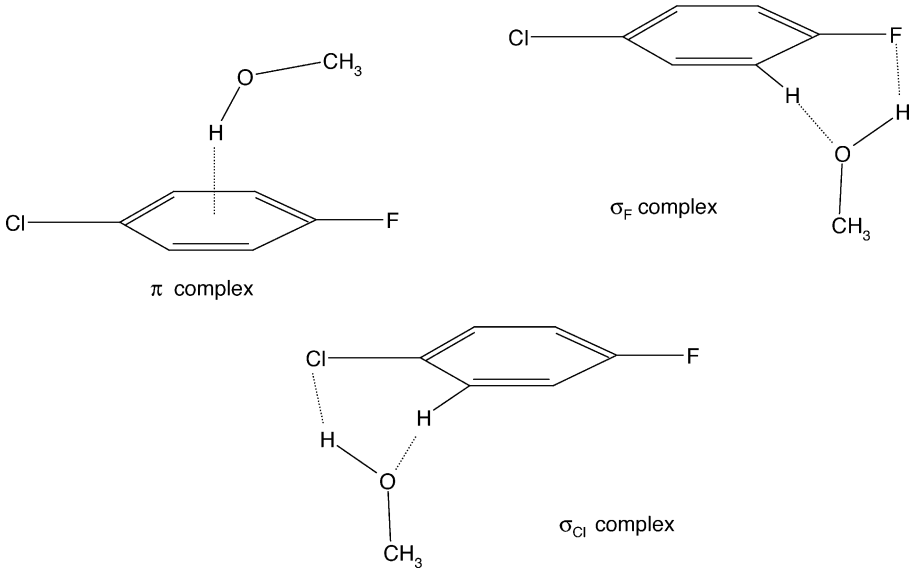

Fig. 8. Characteristic hydrogen-bonded structures of the *p*-chlorofluorobenzene···methanol complex.

and $(CH_3Cl)_2$ and that the B3LYP dimerisation energy of CH_3F is much smaller than the MP2 ones of CH_3Br and CH_3I. On the other hand, a larger dimerisation energy of the heavier halides may be justified by the increased importance of dispersion forces in their dimers on the basis of the larger polarisability of CH_3Br and CH_3I. (The polarisabilities of CH_3X molecules with X = F, Cl, Br and I are 2.97, 5.35, 5.87 and 7.97×10^{-24} cm^3, respectively [61].) Note that a recent MP2/6-31+G(d,p) study of $(CH_3F)_2$ resulted in a dimerisation energy of 5.7 kJ/mol [141]. This value, however, included both BSSE and ZPE corrections in contrast to the BSSE (only)-corrected data of Futami et al. [139]. ZPE can decrease the dimerisation energy of such dimers by a few kJ/mol.

On the basis of the computed frequencies of the monomers and dimers, the head-to-tail conformer was identified in the matrix-isolated spectra in the case of all the four halides. This was the only structure observed for the $(CH_3F)_2$ dimer [139], whereas the spectrum of $(CH_3I)_2$ showed unambiguously the co-existence of the head-to-tail and head-to-head structures [138]. Note that the computed energy difference for the latter two structures was also very small (2.2 kJ/mol). Due to the much weaker secondary features in the spectra of $(CH_3Cl)_2$ and $(CH_3Br)_2$, the head-to-head structure was only tentatively identified in these spectra [140]. In the crystal, both head-to-tail and head-to-head interactions were observed for solid CH_3I [142].

It is worth noting that while the $(CH_3X)_2$ dimers are very weak hydrogen-bonded complexes, the halogen in these molecules can be a very strong proton acceptor. The $CH_3FH^+\cdots FCH_3$ proton bound dimer for example, exhibits a very strong (134 ± 8 kJ/mol) hydrogen bond [143].

Halogen acceptors connected to aromatic carbons are generally involved in complex interactions, as also the aromatic π-system has hydrogen acceptor abilities, comparable to that of the halogens. A representative case is the *p*-chlorofluorobenzene···methanol complex for which MP2/6-31+G(d) calculations resulted in three hydrogen-bonded structures on the potential energy surface: the π complex with O–H···π interaction, the σ_F complex with a $-C_{Ar}-F\cdots H-O(CH_3)\cdots H-C_{Ar}-$ six-ring and the analogous σ_{Cl} complex with a $-C_{Ar}-Cl\cdots H-O(CH_3)\cdots H-C_{Ar}-$ six-ring (cf. Fig. 8) [144]. The BSSE-corrected binding energies were 5.9, 13.7 and 10.8 kJ/mol for the π, σ_F and σ_{Cl} complexes, respectively. Similar results have been obtained for the fluorobenzene···water and *p*-difluorobenzene···water complexes [145]. In the heavier halides (X = Br, I) with weaker HB propensities the π complex may have larger importance at the expense of the σ_X one.

Weak C–H···F–C HB interactions appear in the crystals of fluorobenzenes with H···F distances larger than 2.3 Å. The X-ray diffraction study of fluorobenzene derivatives accompanied by a CSD search for related compounds [146] revealed the strongest interactions among benzene derivatives with the largest number of electronegative substituents, in agreement with the increased acidity of the CH hydrogen.

There are numerous additional examples of C_{Ar}–X···H intermolecular HB, in which the donor is aromatic hydrogen (C_{Ar}–H). Our search in the Cambridge Structural Database (ConQest version 1.6, using searching criteria $H\cdots X \leq \sum$vdW and $C_{Ar}-H\cdots X \geq 130^\circ$, R factor <0.05) resulted in 110, 135 and 35 hits for X = F, Cl and Br, respectively. The distribution of the H···X distances is given in Fig. 9. The H···F distances show a well-defined maximum at 2.55 Å, whereas the H···Cl and H···Br distances have no maximum below the $\sum$vdW value, in agreement with the much weaker character of these interactions.

As noted previously, D–H···X–C contacts have been the subject of several previous CSD analyses and reviews [4,15–24]. In all the cases, the weak HB propensities of organic halogens with respect to O and N acceptors in similar situations were noted. The poor acceptor potential of fluorine attracted particular attention. This behaviour was explained by the low proton affinity and hardness of F (due to its tight electron shell)

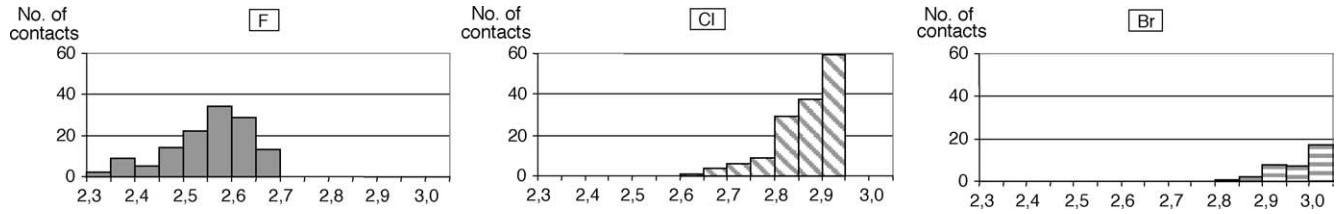

Fig. 9. C_{Ar}–X···H distances from our CSD search using criteria H···X ≤ ∑vdW and C_{Ar}–H···X ≥ 130°.

and by the inability to modify this by intramolecular electron delocalisation or intermolecular cooperative effects [18]. For a comprehensive summary of earlier CSD statistics we refer to the recent book of Desiraju and Steiner [4] including several characteristic examples. Noteworthy is the recent CSD study of van der Berg and Seddon [19], who focussed on the directionality of C–H···X interactions. In addition to the cone correction method they applied an isotropic density correction to correct for both angular and distance effects. The distances of highest incidence from their analysis (with H···X < 7 Å and D–H···X > 90°) were slightly above the ∑vdW distances supporting that HB interactions can extend beyond the classic vdW cut-off criterion.

We terminate this section with a special example of C–H···X–C HB interactions appearing in host-guest systems. Recently, Gibb et al. synthesised new nanoscale hosts functionalised with a crown of weakly acidic benzyl C–H groups [147,148]. From a systematically constructed set of guest (quasi-spherical adamantane) molecules the binding preference of those containing halogen substituents was deduced from experimentally determined association constants. The stronger bonding of the haloderivatives was attributed to the formation of weak tetrafurcated C–H···X–C hydrogen bonds. The strength of bonding increased with the halogen size from X = Cl to I. The X-ray structure of the strongest-bonded host–I···guest adduct revealed H···I distances of 3.077 Å, somewhat below the ∑vdW value of I and H. Estimated HB energies from the association constants taking into account the entropy change of adduct formation indicated a contribution of at least 4 kJ/mol per C–H···I–C hydrogen bond. The total C–H···Br–C and C–H···Cl–C bonding energies of the Br- and Cl-adamantane derivatives were smaller by 15% and 40%, respectively. The decreasing trend from X = I to Cl was attributed to the rigid geometry of the host basket, resulting in less favourable H···X distances when X = Cl and Br [147].

4. Intramolecular hydrogen bonding interactions

The intramolecular HB interactions generally appear in sterically constrained structures. Evaluation of the properties of such HB interactions can be made by comparing the hydrogen-bonded and (if available) non-hydrogen-bonded conformers. In contrast to the intermolecular case, the obtained properties can substantially be influenced by additional intramolecular interactions beside the D–H···X hydrogen bond. These are the repulsion of the lone pairs of D and X in the non-hydrogen-bonded form, the repulsive dipole–dipole interactions between the C–D and C–X dipoles, and, specifically in ethanol derivatives, the attractive gauche effect increasing with the electronegativity of the substituents [149].

In the following we discuss the properties of 2-halophenols and 2-haloethanols, for which the most extensive literature data are available.

4.1. 2-Halophenols

2-Halophenols are probably the first observed examples of intramolecular HB with a halogen acceptor [150]. The HB interaction has been investigated in all the three phases providing extended information on its nature. IR spectroscopy revealed the red-shift of the OH stretching frequency of the hydrogen-bonded *syn* isomers with respect to that of the non-hydrogen-bonded *anti* isomers. In contrast to the expectations based on the general HB strength of the halogens [151,152], the magnitude of the red-shift increases in the order F < Cl < Br < I [153–157] implying the same order for the strength of HB in 2-halophenols. (Note that the small, ca. 20 cm^{-1} splitting of the ν_{OH} band of 2-fluorophenol was recently measured only in non-resonant ionisation detected IR spectroscopy [156] and coherent anti-Stokes Raman experiments [157].) The F < Cl < Br < I behaviour was dubbed as an 'anomalous' order in the strength of the intramolecular hydrogen bond [153].

The enthalpy differences ΔH°, given in Table 6, have been determined on the basis of the ν_{OH} peak areas in the gas-phase IR spectra [154]. The relative stabilities of the two forms were also evaluated from the potential function of the OH internal rotation based on the measured OH torsional frequencies [158]. The two

Table 6
Enthalpy differences (kJ/mol) between the hydrogen-bonded and non-hydrogen-bonded conformers of 2-halophenols and the lengths of the intramolecular hydrogen bonds

	F	Cl	Br	I
ΔH° [a]		14.27 ± 0.59	13.10 ± 1.47	11.51 ± 0.29
ΔH° [b]	6.82	6.82	6.40	5.52
ΔH° [c]	12.68	13.68	13.31	
ΔH° [d]	11.38	12.47	12.93	10.89
X···H [d]	2.231	2.419	2.494	2.630

[a] On the basis of the peak areas in the gas-phase IR spectrum [154].
[b] From the potential function of the OH internal rotation [158].
[c] Computed at the B3LYP/6-31G(d,p) level (X = F, Cl) and at the B3LYP/6-311G(d,p) (X = Br) level including ZPE correction [157].
[d] Computed at the B3LYP/6-311++G(d,p) level including ZPE correction for X = F, Cl, Br [159]. The value for 2-I-phenol was obtained from our B3LYP/6-311++G(d,p) calculations using quasi-relativistic ECP for I [10] extended by single sets of sp diffuse [75] and d-polarisation functions [11].

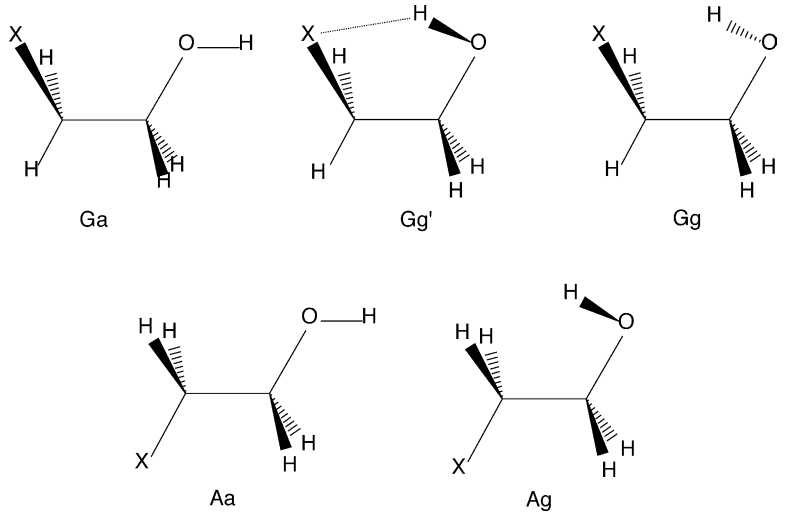

Fig. 10. The five conformers of 2-haloethanols.

sets of enthalpy differences, though differing considerably in magnitude, have the same F > Cl > Br > I order in agreement with the HB propensities of the halogens (cf. Table 6).

From the two theoretical studies on 2-halophenols Shin et al. [157] obtained an order of Cl > Br > F for the energy difference of the two forms (cf. Table 6). Note, however, that the computed energy differences were small, and in such cases the use of a consistent theoretical level for all the compounds is important. (Shin et al. used a basis set for Br different from those of F and Cl.) More consistent data were obtained by Silvi et al. at the B3LYP/6-311++G(d,p) level for X = F, Cl and Br. These calculations reproduced the observed order of red-shifts of the ν_{OH} frequencies, and gave the same order (Br > Cl > F) for the relative stabilities of the two forms (cf. Table 6) [159]. The trend was also supported by the computed geometrical parameters: the O–H bond lengthens the most (0.003 Å) and the O–H···X angle opens the most (to 122.3°) in 2-Br-phenol. No theoretical data are available for 2-I-phenol in the literature. Our B3LYP computations (utilising an ECP basis for I similar in quality to the 6-311+G(d) basis of the other halogens) gave the lowest relative stability for this compound among the 2-halophenols.

The stability order of Br > Cl > F in 2-halophenols might be explained by the geometrical constraints determining the intramolecular HB, as both the OH group and X have very little flexibility. Among the three halogens, the radius of bromine may best accommodate the constraints, hence the most advanced interaction may appear with Br. It should be kept in mind, however, that ambiguities might appear in both the experimental and computed data. The computed small energy differences, particularly those between 2-Cl- and 2-Br-phenol, can change by going to higher levels of theory. On the other hand, in the experimental study uncertainties may stem from the separation of the bands of the two isomers, from the integration of the weak band of the anti conformer in the IR spectra [154] and from the assumed identical absorption coefficient of the two forms. Regarding the study of Carlson et al. [158], the torsional frequencies can be determined accurately. Here the approximations used in the potential function model introduce some uncertainty. Nevertheless, taking into account the experimental errors of the enthalpy differences by Lin and Fishman [154], their data do not contradict with the computed enthalpy differences of Silvi et al. [159] for X = Cl and Br, neither with our obtained value for 2-I-phenol.

Finally, we note the effect of repulsion of the lone pairs of O and X on the relative stabilities of the two conformers. With increasing halogen size the anti conformer is more destabilised due to the larger repulsion of the lone pairs. This additional support to the larger relative stability of the hydrogen-bonded conformer in the heavier halides has no relation to the HB interaction and is difficult to assess.

4.2. 2-Haloethanols

2-Haloethanols represent a more complex system due to the five possible conformers based on the internal rotation around the CC and CO axes (cf. Fig. 10). From them, the only conformer containing HB interaction is Gg′. The energy difference between the G conformers can be a reasonable estimate of the HB energy, as the gauche and dipole–dipole interactions are present in all the three G conformers, whereas the HB in Gg′ is replaced by a steric interaction between the lone pairs of O and X in Ga and Gg. From the latter two conformers, Gg shows a smaller steric effect, therefore it is better suited to estimate the HB energy. The steric interaction is not present in the A conformers, but also the other contributions vanish. In general, the A conformers have lower energies than the Ga and Gg ones and are most likely the minor components in gas-phase experiments.

2-Haloethanols have been investigated by electron diffraction and microwave spectroscopy, and the hydrogen-bonded Gg′ conformers were identified as the major component in the gas phase [160–164]. The co-existence of two-three conformers has been reported on the basis of the gas-phase IR spectra of 2-Cl-, 2-Br- and 2-I-ethanol. The small differences in the OH stretching frequencies of the conformers (between 20 and 60 cm^{-1}) [165,166] are indicative of weak HB interactions. In the case of 2-F-ethanol, both the gas-phase and xenon-solution IR spectra showed the presence of a single (the most stable Gg′) conformer.

Table 7
Enthalpy differences (kJ/mol) of the hydrogen-bonded and non-hydrogen-bonded conformers of 2-haloethanols and the lengths of the intramolecular hydrogen bonds

	F	Cl	Br	I
ΔH°		4.98 ± 0.42[a], 5.02 ± 0.42[b]	3.76 ± 0.48[c], 6.07 ± 0.42[b]	3.7 ± 2.9[d]
ΔH	9.4[e]	4.5[f]	7.6[g], 6.3[f]	6.5[g]
X···H	2.489 ± 0.039[h]	2.6092 ± 0.0020[i]	2.705 ± 0.010[i]	3.002 ± 0.056[d]

[a] From the IR spectrum of the xenon solution [168].
[b] From temperature variable (20–165 °C) infrared measurements of the vapour utilising the CX stretching bands [165].
[c] From the IR spectrum of the xenon solution with respect to the Ag conformer [169]. The Aa conformer was also identified in the IR spectrum with a relative stability of 4.49 ± 0.48 kJ/mol.
[d] From gas-phase electron diffraction [162].
[e] From computations at the MP2/6-311++G(d,p) level without ZPE-correction [167].
[f] From MP2/6-31++G(d,p) calculations including ZPE corrections [170]. The relative stability of the Ag conformer of 2-Cl-ethanol was computed to be 5.6 kJ/mol, that of the Aa conformer of 2-Br-ethanol to 7.2 kJ/mol. The Ga conformers were computed to be less stable than Gg′ by 7.8 and 9.3 kJ/mol for Cl- and Br-ethanol, respectively.
[g] Energy difference between the Gg′ and Aa conformers from present MP2/6-311++G(d,p) calculations using quasi-relativistic ECP for Br and I [10,11] applying corrections for ZPE.
[h] From gas-phase electron diffraction (r_g parameter) [163].
[i] From microwave spectroscopy [164].

The only information on its HB energy comes from MP2/6-311++G(d,p) computations [167] (cf. Table 7).

Among 2-haloethanols the Cl- and Br-derivatives have been investigated extensively by experimental and theoretical methods. The relative stability between Gg′ and the anti forms of 2-Cl-ethanol has been determined from the IR spectrum of both the gas phase [165] and xenon solution [168]. In a recent analysis of the IR spectrum of 2-Br-ethanol dissolved in liquid xenon the Ag and Aa conformers have been observed. The enthalpy differences relative to Gg′ have been determined by variable temperature studies between −63 and −100 °C and by quantum chemical calculations at the MP2/6-311+G(d,p) level (cf. Table 7) [169]. The latter experimental value is somewhat lower than that obtained from early variable temperature (20–130 °C) infrared measurements of the vapour (6.07 ± 0.42 kJ/mol between two unassigned conformers, cf. Table 7) [165].

Recently, quantum chemical calculations have been performed on the whole conformational space of 2-Cl- and 2-Br-ethanol at the MP2/6-31++G(d,p) and B3LYP/6-31++G(d,p) levels [170]. The relative stability of the most stable 2-Cl-ethanol conformer agrees well with the experimental value of Durig et al. [169]. On the other hand, the computed ΔH of 2-Br-ethanol is almost two-times larger than the value derived from the spectrum of the xenon solution [169], while it agrees with ΔH° from the early vapour-phase IR measurement of Buckley et al. [165] (cf. Table 7).

The only structural study of 2-I-ethanol was performed by Thomassen et al. using gas-phase electron diffraction (together with a study of 2-Br-ethanol) [162]. From variable temperature measurements a rough estimate of the energy difference between the hydrogen-bonded and non-hydrogen-bonded conformers was 7.6 ± 2.7 and 3.7 ± 2.9 kJ/mol for Br- and I-ethanol, respectively. Our MP2 calculations gave a much higher relative stability (6.5 kJ/mol) of the Gg′ conformer of 2-I-ethanol with respect to the Aa conformer.

The experimental and computed hydrogen-bond lengths given in Table 7 are close to the $\sum$vdW distances (particularly those of X = Cl, Br and I), as another indications of weak interactions. Comparing the two presented intramolecular hydrogen-bonded systems, the HB in 2-halophenols is two to three times stronger due primarily to the more suited geometrical arrangements of the OH and X groups.

5. Conclusions

In the present review, we performed a comparative assessment of HB interactions with halogen (X) acceptors based on data available in the literature. Four main acceptor types

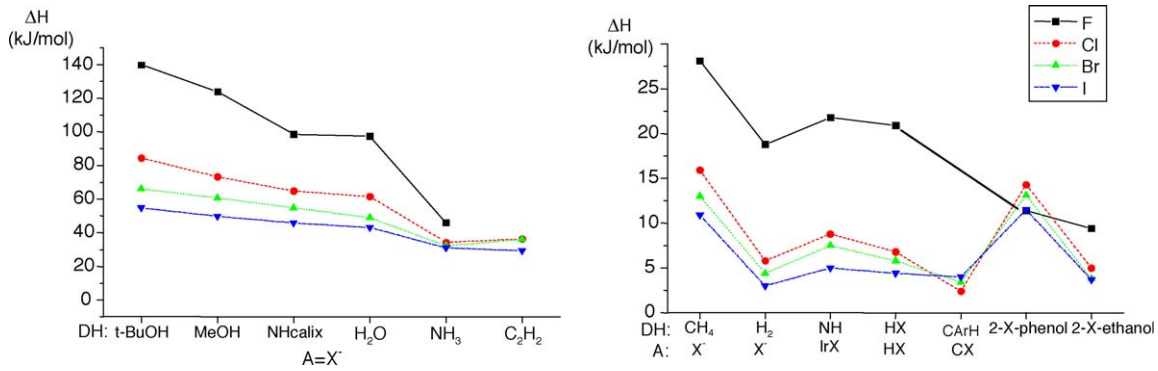

Fig. 11. Overview of characteristic HB energies (DH = donor; A = acceptor; X = F, Cl, Br, I).

have been considered, viz., free X^- anions, halogens in M–X (M = transition metal), H–X and C–X bonds. Among the molecular properties we focussed on the HB energy and structural characteristics that are particularly informative on the HB propensities of the halogens.

In Fig. 11, an overview of the most characteristic HB energies (obtained from experiment or computations) is presented. Obvious is the very strong hydrogen bond with anionic halogen (X^-) acceptors, the strongest interaction appearing with the *t*-BuOH donor. The HB energies fall below 30 kJ/mol in the case of the weak CH_4 and H_2 donors. The very weak $H_2\cdots X^-$ interactions are comparable in magnitude with the HX···HX and C_{Ar}–H···X–C hydrogen bonds.

Literature data on H···X–M and H···X–C interactions include mainly the geometrical parameters determined by diffraction methods, while information on the HB energies of such systems is very rare. The mean H···X distances evaluated by CSD studies indicate generally weak interactions if the donor is C–H and/or X = I, otherwise medium and, particularly with X = F, strong ones.

Most HB systems show a trend of F > Cl > Br > I for the HB strength. Exceptions appear in the case of rigid systems (e.g., nanoscale host–guest ones) where the steric constraints can lead to preferred interactions with the larger halogens. Note, however, that in these weak interactions the differences in the HB energies of different X acceptors are very small.

Acknowledgements

Financial support from the Hungarian Scientific Research Foundation (OTKA No. T046183) and computational time from the National Information Infrastructure Development Program of Hungary is gratefully acknowledged. A.K. thanks the Bolyai Foundation for support.

References

[1] M.L. Huggins, Angew. Chem. Int. Ed. 10 (1971) 147.
[2] G.A. Jeffrey, An Introduction to Hydrogen Bonding, Oxford University Press, Oxford, 1997.
[3] L. Pauling, J. Am. Chem. Soc. 53 (1931) 1367.
[4] G.R. Desiraju, T. Steiner, The Weak Hydrogen Bond in Structural Chemistry and Biology, Oxford University Press, Oxford, 1999.
[5] G.A. Jeffrey, W. Saenger, Hydrogen Bonding in Biological Structures, Springer-Verlag, Berlin, 1991.
[6] M.D. Joesten, L.J. Schaad, Hydrogen Bonding, Dekker, New York, 1974.
[7] S. Scheiner, Hydrogen Bonding. A Theoretical Perspective, Oxford University Press, Oxford, 1997.
[8] T. Steiner, G.R. Desiraju, Chem. Commun. (1998) 891.
[9] M.J. Frisch, G.W. Trucks, H.B. Schlegel, G.E. Scuseria, M.A. Robb, J.R. Cheeseman, V.G. Zakrzewski, J.A. Montgomery Jr., R.E. Stratmann, J.C. Burant, S. Dapprich, J.M. Millam, A.D. Daniels, K.N. Kudin, M.C. Strain, O. Farkas, J. Tomasi, V. Barone, M. Cossi, R. Cammi, B. Mennucci, C. Pomelli, C. Adamo, S. Clifford, J. Ochterski, G.A. Petersson, P.Y. Ayala, Q. Cui, K. Morokuma, A.D. Rabuck, K. Raghavachari, J.B. Foresman, J. Cioslowski, J.V. Ortiz, B.B. Stefanov, G. Liu, A. Liashenko, P. Piskorz, I. Komaromi, R. Gomperts, R.L. Martin, D.J. Fox, T. Keith, M.A. Al-Laham, C.Y. Peng, A. Nanayakkara, C. Gonzalez, M. Challacombe, P.M.W. Gill, B. Johnson, W. Chen, M.W. Wong, J.L. Andres, C. Gonzalez, M. Head-Gordon, E.S. Replogle, J.A. Pople, Gaussian '98, Gaussian Inc., Pittsburgh, PA, 1998.
[10] A. Bergner, M. Dolg, W. Küchle, H. Stoll, H. Preuss, Mol. Phys. 80 (1993) 1431.
[11] J. Andzelm, S. Huzinaga, M. Klobukowski, E. Radzio, Y. Sakai, H. Tatekawi, Gaussian Basis Sets for Molecular Calculations, Elsevier, Amsterdam, 1984.
[12] T. Steiner, Angew. Chem. Int. Ed. 41 (2002) 48.
[13] M.M. Meot-Ner, S.G. Lias, in: P.J. Linstrom, W.G. Mallard (Eds.), NIST Chemistry WebBook, NIST Standard Reference Database Number 69, National Institute of Standards and Technology, Gaithersburg, MD, 2001.
[14] F.H. Allen, Acta Crystallogr. B 58 (2002) 380.
[15] P. Murray-Rust, W.C. Stalling, C.T. Monti, R.K. Preston, J.P. Glusker, J. Am. Chem. Soc. 105 (1983) 3206.
[16] L. Shimoni, J.P. Glusker, Struct. Chem. 5 (1994) 383.
[17] J.A.K. Howard, V.J. Hoy, D. O'Hagan, G.T. Smith, Tetrahedron 52 (1996) 12613.
[18] J.D. Dunitz, R. Taylor, Chem. Eur. J. 3 (1997) 89.
[19] J.-A. van der Berg, K.R. Seddon, Cryst. Growth Design 5 (2003) 643.
[20] R. Ahuja, A.G. Samuelson, Cryst. Eng. Commun. 5 (2003) 395.
[21] G. Aullón, D. Bellamy, L. Brammer, E. Bruton, A.G. Orpen, Chem. Commun. (1998) 653.
[22] D. Braga, S.M. Draper, E. Champeil, F. Grepioni, J. Organomet. Chem. 573 (1999) 73.
[23] C.B. Aakeroy, T.A. Evans, K.R. Seddon, I. Palinko, N. J. Chem. 23 (1999) 145.
[24] P.K. Thallapally, A. Nangia, Cryst. Eng. Commun. 27 (2001) 1.
[25] L. Brammer, E.A. Bruton, P. Sherwood, N. J. Chem. 23 (1999) 965.
[26] F. Neve, A. Crispini, Cryst. Growth Design 1 (2001) 387.
[27] G. Gilli, P. Gilli, J. Mol. Struct. 552 (2000) 1.
[28] L.J. Bellamy, A.J. Owens, Spectrochim. Acta 25A (1969) 329.
[29] M. Rozenberg, A. Loewenschuss, Y. Marcus, Phys. Chem. Chem. Phys. (2000) 2699.
[30] P. Hobza, Z. Havlas, Chem. Rev. 100 (2000) 4253.
[31] G. Caldwell, P. Kebarle, J. Am. Chem. Soc. 106 (1984) 967.
[32] K. Hiraoka, S. Mizuse, S. Yamabe, J. Phys. Chem. 92 (1988) 3943.
[33] J.W. Larson, T.B. McMahon, Inorg. Chem. 23 (1984) 2029.
[34] M.S. Johnson, K.T. Kuwata, C.-K. Wong, M. Okumura, Chem. Phys. Lett. 260 (1996) 551.
[35] D.A. Wild, E.J. Bieske, Int. Rev. Phys. Chem. 22 (2003) 129.
[36] J.L. Finney, Acta Crystallogr. B 51 (1995) 447.
[37] J. Kroon, J.A. Kanters, Nature 248 (1974) 667.
[38] F. Jensen, Introduction to Computational Chemistry, Wiley, New York, 1999.
[39] C.J. Cramer, Essentials of Computational Chemistry, Wiley, New York, 2002.
[40] H. Umeyama, K. Morokuma, J. Am. Chem. Soc. 99 (1977) 1316.
[41] P.A. Kollman, L.C. Allen, Chem. Rev. 72 (1972) 283.
[42] C. Moller, M.S. Plesset, Phys. Rev. 46 (1934) 618.
[43] J.E. Del Bene, I. Shavitt, in: S. Scheiner (Ed.), Intermolecular Interactions: From van der Waals to Strongly Bound Complexes, Wiley, Sussex, 1997.
[44] J.E. Del Bene, in: P.V.R. Schleyer, N.L. Allinger, T. Clark, J. Gasteiger, P.A. Kollman, H.F. Schaefer III, P.R. Schreiner (Eds.), The Encyclopedia of Computational Chemistry, vol. 2, Wiley, Chichester, UK, 1998.
[45] A.D. Becke, J. Chem. Phys. 98 (1993) 5648.
[46] W. Koch, M.C. Holthausen, A Chemist's Guide to Density Functional Theory, Wiley/VCH, Weinheim, 2002, p. 213.
[47] C. Lee, W. Yang, R.G. Parr, Phys. Rev. B 37 (1988) 785.
[48] S. Kristyán, P. Pulay, Chem. Phys. Lett. 229 (1994) 175.
[49] W.R. Wadt, P.J. Hay, J. Chem. Phys. 82 (1985) 284.
[50] A.W. Ehlers, M. Böhme, S. Dapprich, A. Gobbi, A. Höllwarth, V. Jonas, K.F. Köhler, R. Stegmann, A. Veldkamp, G. Frenking, Chem. Phys. Lett. 208 (1993) 111.
[51] A. Höllwarth, M. Böhme, S. Dapprich, A.W. Ehlers, A. Gobbi, V. Jonas, K.F. Köhler, R. Stegmann, A. Veldkamp, G. Frenking, Chem. Phys. Lett. 208 (1993) 237.

[52] M. Hargittai, I. Hargittai, Int. J. Quantum Chem. 44 (1992) 1057.
[53] S. Berski, Z. Latajka, Int. J. Quantum Chem. 90 (2002) 1108.
[54] A. Savin, A.D. Becke, J. Flad, R. Nesper, H. Preuss, H.G. von Schnering, Angew. Chem. Int. Ed. 30 (1991) 409.
[55] G. Fuster, B. Silvi, Theor. Chem. Acc. 104 (2000) 13.
[56] P.G. Wenthold, R.R. Squires, J. Phys. Chem. 99 (1995) 2002.
[57] G. Caldwell, P. Kebarle, Can. J. Chem. 63 (1985) 1399.
[58] J.E. Del Bene, Spectrochim. Acta 55A (1999) 719.
[59] K. Kawaguchi, E. Hirota, J. Chem. Phys. 87 (1987) 6838.
[60] K. Kawaguchi, J. Chem. Phys. 88 (1988) 4186.
[61] D.R. Lide (Ed.), CRC Handbook of Chemistry and Physics, 83rd ed., CRC Press, Boca Raton, USA, 2002.
[62] A. Bondi, J. Chem. Phys. 68 (1964) 441.
[63] M. Arshadi, R. Yamdagni, P. Kebarle, J. Phys. Chem. 74 (1970) 1475.
[64] S.S. Xantheas, T.H. Dunning Jr., J. Phys. Chem. 98 (1994) 13489.
[65] J.H. Choi, K.T. Kuwata, Y.B. Cao, M. Okumura, J. Phys. Chem. A 102 (1998) 503.
[66] J. Kim, H.M. Lee, S.B. Suh, D. Majumdar, K.S. Kim, J. Chem. Phys. 113 (2000) 5259.
[67] B.J. Howard, T.R. Dyke, W. Klemperer, J. Chem. Phys. 81 (1984) 5417.
[68] B. Bogdanov, M. Peschke, D.S. Tonner, J.E. Szulejko, T.B. McMahon, Int. J. Mass Spectrom. 187 (1999) 707.
[69] B. Bogdanov, T.B. McMahon, J. Phys. Chem. A 104 (2000) 7871.
[70] F.K.J. Tanabe, N.H. Morgon, J.M. Riveros, J. Phys. Chem. 100 (1996) 2862.
[71] D.H. Evans, R.G. Keesee, A.W. Castleman Jr., J. Chem. Phys. 86 (1987) 2927.
[72] P.S. Weiser, D.A. Wild, P.P. Wolynec, E.J. Bieske, J. Phys. Chem. A 104 (2000) 2562.
[73] P. Botschwina, T. Dutoi, M. Mladenović, R. Oswald, S. Schmatz, H. Stoll, Faraday Discuss. 118 (2001) 433.
[74] D.A. Wild, P.J. Milley, Z.M. Loh, P.P. Wolynec, P.S. Weiser, E.J. Bieske, J. Chem. Phys. 113 (2000) 1075.
[75] P. Botschwina, H. Stoll, Phys. Chem. Chem. Phys. 3 (2001) 1965.
[76] K. Hiraoka, T. Mizuno, T. Iiono, D. Eguchi, S. Yamabe, J. Phys. Chem. A 105 (2001) 4887.
[77] B. Hartke, H.J. Werner, Chem. Phys. Lett. 280 (1997) 430.
[78] A.I. Boldyrev, J. Simons, G.V. Mil'nikov, V.A. Benderskii, S.Y. Grebenshchikov, E.V. Vetoshkin, J. Chem. Phys. 102 (1995) 1295.
[79] Z. Latajka, J. Mol. Struct. (Theochem.) 85 (1992) 225.
[80] S. Irle, J.M. Bowman, J. Chem. Phys. 113 (2000) 8401.
[81] M. Masamura, J. Chem. Phys. 118 (2003) 6336.
[82] J. Baik, J. Kim, D. Majumdar, K.S. Kim, J. Chem. Phys. 110 (1999) 9116.
[83] M. Masamura, J. Phys. Chem. A 106 (2002) 8925.
[84] H.M. Lee, K.S. Kim, J. Chem. Phys. 114 (2001) 4461.
[85] W.H. Robertson, K. Karapetian, P. Ayotte, K.D. Jordan, M.A. Johnson, J. Chem. Phys. 116 (2002) 4853.
[86] G. Markovich, O. Cheshnovsky, U. Kaldor, J. Chem. Phys. 99 (1993) 6201.
[87] M. Roy, T.B. McMahon, Can. J. Chem. 63 (1985) 708.
[88] J.J. Rabasco, S.R. Kass, J. Am. Soc. Mass Spectrom. 3 (1992) 91.
[89] M.-L.H. Jeng, B.S. Ault, J. Phys. Chem. 95 (1991) 2687.
[90] A.C. Simmonett, S.E. Wheeler, H.F. Schaefer III, J. Phys. Chem. A 108 (2004) 1608.
[91] P.S. Weiser, D.A. Wild, E.J. Bieske, J. Chem. Phys. 110 (1999) 9443.
[92] P.S. Weiser, D.A. Wild, E.J. Bieske, Chem. Phys. Lett. 299 (1999) 303.
[93] J.J. Novoa, M.-H. Whangbo, J.M. Williams, Chem. Phys. Lett. 180 (1991) 241.
[94] D.A. Wild, Z.M. Loh, P.P. Wolynec, P.S. Weiser, E.J. Bieske, Chem. Phys. Lett. 332 (2000) 531.
[95] D.A. Wild, Z.M. Loh, E.J. Bieske, Int. J. Mass Spectrom. 220 (2002) 273.
[96] P. Ayotte, G.H. Weddle, J. Kim, M.A. Johnson, J. Am. Chem. Soc. 120 (1998) 12361.
[97] P. Ayotte, J.A. Kelley, S.B. Nielsen, M.A. Johnson, Chem. Phys. Lett. 316 (2000) 455.
[98] D.A. Wild, P.S. Weiser, E.J. Bieske, A. Zehnacker, J. Chem. Phys. 115 (2001) 824.
[99] D.A. Wild, Z.M. Loh, R.L. Wilson, E.J. Bieske, J. Chem. Phys. 117 (2002) 3256.
[100] D.A. Wild, R.L. Wilson, Z.M. Loh, E.J. Bieske, Chem. Phys. Lett. 393 (2004) 517.
[101] D.A. Wild, P.S. Weiser, Z.M. Loh, E.J. Bieske, J. Phys. Chem. A 106 (2002) 906.
[102] T. Steiner, Acta Crystallogr. B 54 (1998) 456.
[103] R.D. Shannon, Acta Crystallogr. A 32 (1976) 751.
[104] T. Steiner, J. Mol. Struct. 443 (1998) 149.
[105] P.A. Gale, J.L. Sessler, V. Král, V. Lynch, J. Am. Chem. Soc 118 (1996) 5140.
[106] P.A. Gale, Coord. Chem. Rev. 213 (2001) 79.
[107] P.A. Gale, P. Anzenbacher, J.L. Sessler, Coord. Chem. Rev. 222 (2001) 57.
[108] Y.D. Wu, D.F. Wang, J.L. Sessler, J. Org. Chem. 66 (2001) 3739.
[109] A.F.D. de Namor, M. Shehab, J. Phys. Chem. B 107 (2003) 6462.
[110] D.F. Wang, Y.D. Wu, Arkivoc Part 9 (2004) 96.
[111] F. Pichierri, J. Mol. Struct. (Theochem.) 581 (2002) 117.
[112] E. Peris, J.C. Lee, J.R. Rambo, O. Eisenstein, R.H. Crabtree, J. Am. Chem. Soc. 117 (1995) 3485.
[113] T.R. Dyke, B.J. Howard, W. Klemperer, J. Chem. Phys. 56 (1972) 2442.
[114] C. Andreani, M. Nardone, F.P. Ricci, A.K. Soper, Phys. Rev. A 46 (1992) 4709.
[115] J. Zhang, M. Dulligan, J. Segall, Y. Wen, C. Witting, J. Phys. Chem. 99 (1995) 13680.
[116] A. Engdahl, B. Nelander, J. Phys. Chem. 90 (1986) 6118.
[117] G.A. Blake, K.L. Busarow, R.C. Cohen, K.B. Laughlin, Y.T. Lee, R.J. Saykally, J. Chem. Phys. 89 (1988) 6577.
[118] W.J. Lafferty, R.D. Suenram, F.J. Lovas, J. Mol. Spectrosc. 123 (1987) 434.
[119] M.D. Schuder, C.M. Lovejoy, R. Lascola, D.J. Nesbitt, J. Chem. Phys. 99 (1993) 4346.
[120] J.F. Gaw, Y. Yamaguchi, M.A. Vincent, H.F. Schaefer, J. Am. Chem. Soc. 106 (1984) 3133.
[121] Y. Hannachi, B. Silvi, J. Mol. Struct. (Theochem.) 200 (1989) 483.
[122] Z. Latajka, S. Scheiner, Chem. Phys. 216 (1997) 37.
[123] A.S. Pine, B.J. Howard, J. Chem. Phys. 84 (1986) 590.
[124] M.J. Frisch, J.E. Del Bene, J.S. Binkley, H.F. Schaefer, J. Chem. Phys. 84 (1986) 2279.
[125] J. Obriot, F. Fondere, P. Marteau, J. Chem. Phys. 85 (1986) 4925.
[126] A.J. Barnes, J.B. Davies, H.E. Hallam, J.D.R. Howells, Faraday Trans. 2 69 (1973) 246.
[127] R.E. Bumgarner, S.G. Kukolich, J. Chem. Phys. 86 (1987) 1083.
[128] L. Andrews, R.B. Bohn, J. Chem. Phys. 90 (1989) 5205.
[129] A. Engdahl, B. Nelander, J. Phys. Chem. 94 (1990) 8777.
[130] D. Maillard, A. Schriver, J.P. Perchard, C. Giradet, J. Chem. Phys. 71 (1979) 505.
[131] R.B. Bohn, R.D. Hunt, L. Andrews, J. Phys. Chem. 93 (1989) 3979.
[132] K.D. Kolenbrander, C.E. Dykstra, J.M. Lisy, J. Chem. Phys. 88 (1988) 5995.
[133] H. Sun, R.O. Watts, U. Buck, J. Chem. Phys. 96 (1992) 1810.
[134] D. Luckhaus, M. Quack, U. Schmitt, M.A. Suhm, Ber. Bunsenges. Phys. Chem. 99 (1995) 457.
[135] S.-Y. Liu, D.W. Michel, C.E. Dykstra, J.M. Lisy, J. Chem. Phys. 84 (1986) 5032.
[136] Z. Latajka, S. Scheiner, Chem. Phys. 122 (1988) 413.
[137] R.C. Guedes, P.C. do Couto, B.J. Costa Cabral, J. Chem. Phys. 118 (2003) 1272.
[138] F. Ito, T. Nakanaga, Y. Futami, S. Kudoh, M. Takayanagi, M. Nakata, Chem. Phys. Lett. 343 (2001) 185.
[139] Y. Futami, S. Kudoh, M. Takayanagi, M. Nakata, Chem. Phys. Lett. 357 (2002) 209.

[140] Y. Futami, S. Kudoh, F. Ito, T. Nakanaga, M. Nakata, J. Mol. Struct. 690 (2004) 9.
[141] E. Kryachko, S. Scheiner, J. Phys. Chem. A 108 (2004) 2527.
[142] T. Kawaguchi, M. Hijikigawa, Y. Hayafuji, M. Ikeda, R. Fukushima, Y. Tomiie, Bull. Chem. Soc. Jpn. 46 (1973) 53.
[143] T.B. McMahon, P. Kebarle, J. Am. Chem. Soc. 108 (1986) 6502.
[144] C. Riehn, K. Buchhold, B. Reimann, S. Djafari, H.-D. Barth, B. Brutschhy, P. Tarakeshwar, K.S. Kim, J. Chem. Phys. 112 (2000) 1170.
[145] P. Tarakeshwar, K.S. Kim, B. Brutschhy, J. Chem. Phys. 110 (1999) 8501.
[146] V.R. Thalladi, H.-C. Weiss, D. Bläser, R. Boese, A. Nangia, G.R. Desiraju, J. Am. Chem. Soc. 120 (1998) 8702.
[147] C.L.D. Gibb, E.D. Stevens, B.C. Gibb, J. Am. Chem. Soc. 123 (2001) 5849.
[148] Z.R. Laughrey, C.L.D. Gibb, T. Senechal, B.C. Gibb, Chem. Eur. J. 9 (2003) 130.
[149] A.J. Kirby, The Anomeric Effect and Related Stereoelectronic effects at Oxygen, Springer-Verlag, Berlin, 1983, p. 32.
[150] L. Pauling, J. Am. Chem. Soc. 58 (1936) 94.
[151] G.C. Pimentel, A.L. McClellan, The Hydrogen Bond, Freeman, San Francisco, 1960.
[152] P. Schuster, G. Zundel, C. Sandorfy, The Hydrogen Bond: Recent Developments in Theory and Experiments, North Holland, Amsterdam, 1976.
[153] H. Bourassa-Bataille, P. Sauvageau, C. Sandorfy, Can. J. Chem. 41 (1963) 2240.
[154] T. Lin, E. Fishman, Spectrochim. Acta 23A (1967) 491.
[155] E.A. Robinson, H.D. Schreiber, J.N. Spencer, Spectrochim. Acta 28A (1972) 397.
[156] T. Omi, H. Shitami, N. Sekiya, K. Takazawa, M. Fujii, Chem. Phys. Lett. 252 (1996) 287.
[157] D.N. Shin, J.W. Hahn, K.-H. Jung, T.-K. Ha, J. Raman Spectrosc. 29 (1998) 245.
[158] G.L. Carlson, W.G. Fataley, A.S. Manocha, F.F. Bentley, J. Phys. Chem. 76 (1971) 1553.
[159] B. Silvi, E.S. Kryachko, O. Tishchenko, F. Fuster, M.T. Nguyen, Mol. Phys. 100 (2002) 1659.
[160] K.S. Buckton, R.G. Azrak, J. Chem. Phys. 52 (1970) 5652.
[161] R.G. Azrak, E.B. Wilson, J. Chem. Phys. 52 (1970) 5299.
[162] H. Thomassen, S. Samdal, K. Hedberg, J. Phys. Chem. 97 (1993) 4004.
[163] J. Huang, K. Hedberg, J. Am. Chem. Soc. 111 (1989) 6909.
[164] R.G. Azrak, E.B. Wilson, J. Chem. Phys. 52 (1970) 5299.
[165] P. Buckley, P. Giguere, M. Schneider, Can. J. Chem. 47 (1969) 901.
[166] L. Homanen, Spectrochim. Acta 39A (1983) 77.
[167] T.K. Gounev, S. Bell, L. Zhou, J.R. Durig, J. Mol. Struct. 447 (1998) 21.
[168] J.R. Durig, L. Zhou, T.K. Gounev, P. Klaeboe, G.A. Guirgis, L.-F. Wang, J. Mol. Struct. 385 (1996) 7.
[169] J.R. Durig, S. Shen, G.A. Guirgis, J. Mol. Struct. 560 (2001) 295.
[170] S.X. Tian, N. Kishimoto, K. Ohno, J. Phys. Chem. A 107 (2003) 53.